Robotic Spacecraft Rendezvous with a Tumbling Target for Capture: Robust Methods for Planning and Control

Dr. Roberto Lampariello
Leader of On-Orbit Servicing Operations and Validation Team
Institute of Robotics and Mechatronics
German Aerospace Center (DLR)

Plateau de Saclay Automatic Control Seminar
Laboratory of Signals and Systems (L2S)
CNRS, Centrale Supélec and
University of Paris-Saclay
14th March 2024

DLR

Three Goals in Orbital Robotics

- On-orbit servicing
  - Approaching, grasping and stabilizing defective non-cooperative tumbling satellites *for repair*

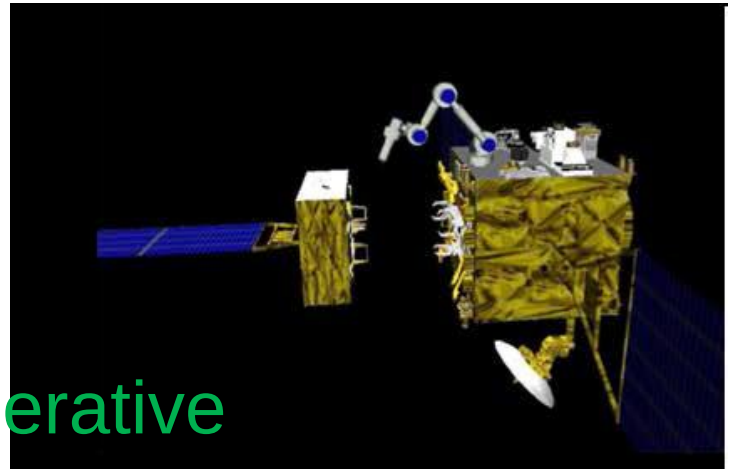

ETS-VII Mission (JAXA) - 1998

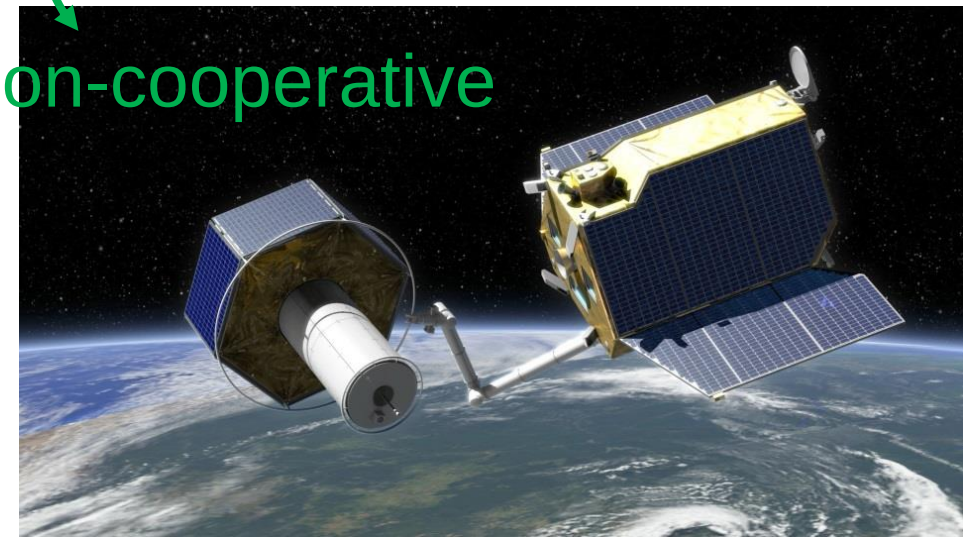

DEOS mission study (DLR) - 2015

Three Goals in Orbital Robotics

- On-orbit servicing
  - Approaching, grasping and stabilizing defective non-cooperative tumbling satellites *for repair*
  - Heading towards life-extension, on-orbit assembly, reconfiguration

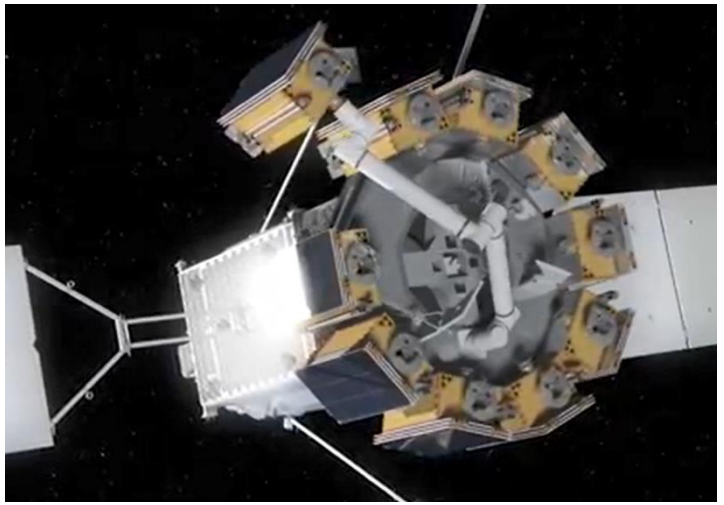

Life-extension concept Northrop Grumman

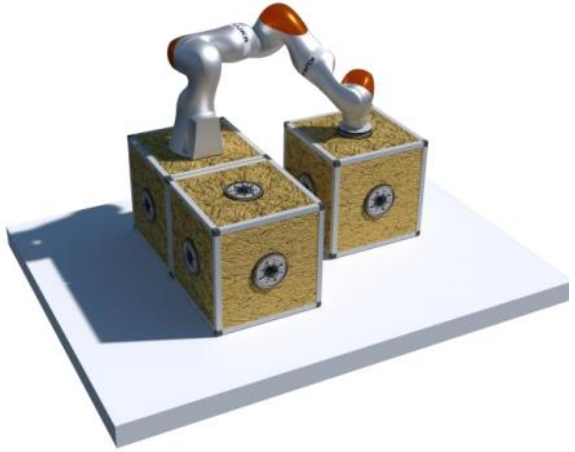

Reconfiguration EU Projects
MOSAR, ORU-BOAS (2020-23)

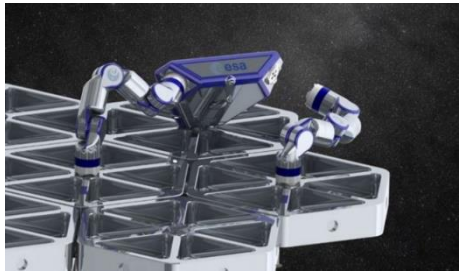

MIRROR
ESA, 2020-22

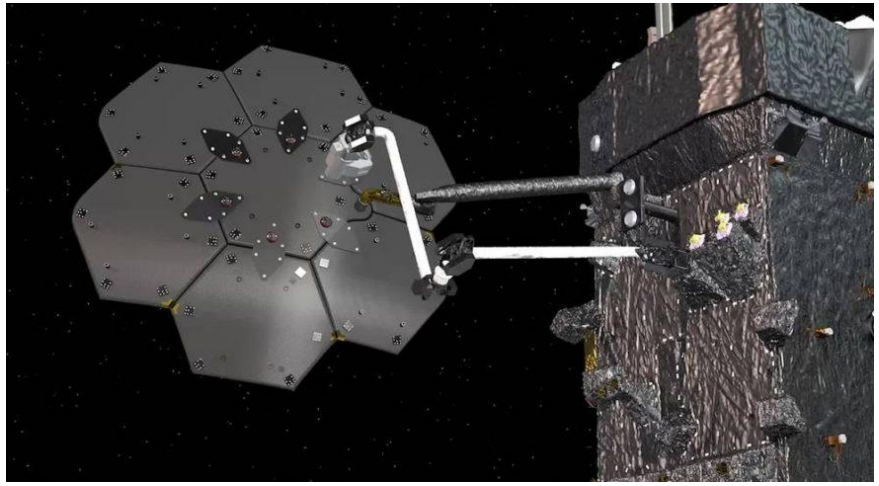

OSAM-1 (NASA, cancelled)

Three Goals in Orbital Robotics

- On-orbit servicing
- Active Debris Removal
  - Approaching, grasping and stabilizing defective non-cooperative tumbling satellites *for deorbiting*

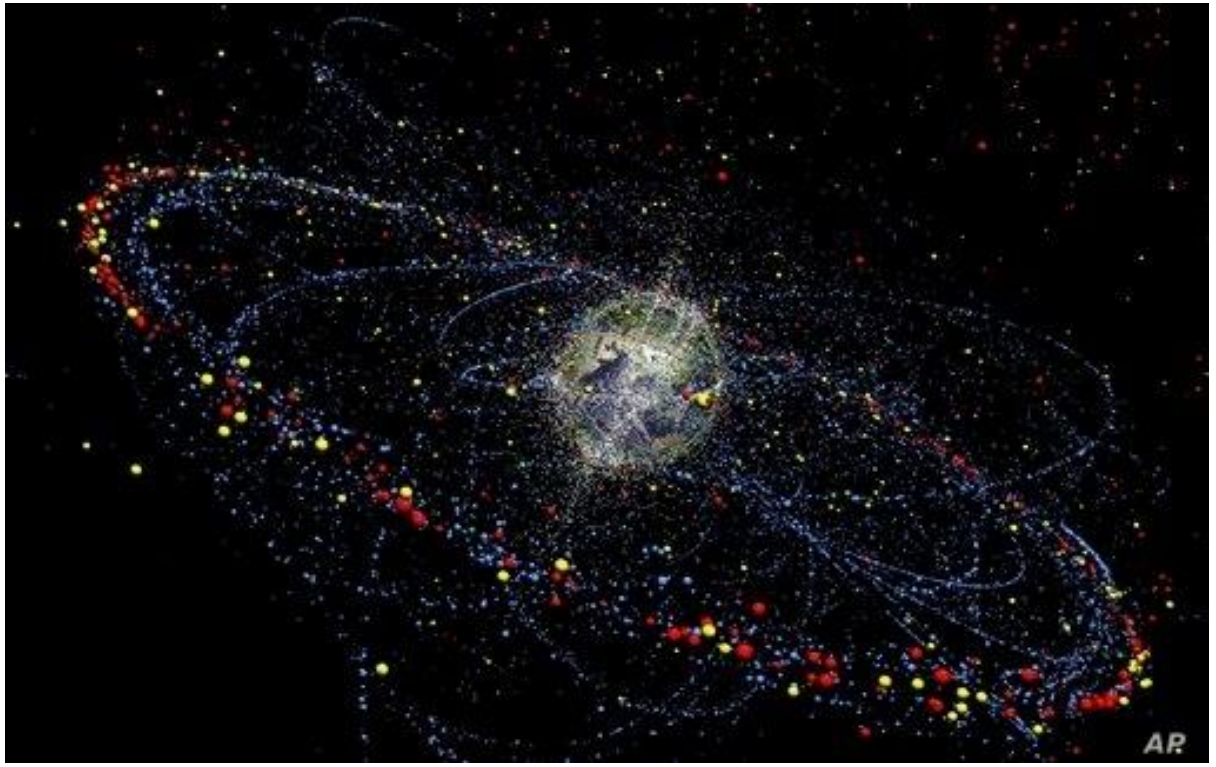

Space debris in Earth orbit

Three Goals in Orbital Robotics

- On-orbit servicing
- Active Debris Removal
  - Approaching, grasping and stabilizing defective non-cooperative tumbling satellites *for deorbiting*
  - New challenges: flight synchronization and communication link obstruction

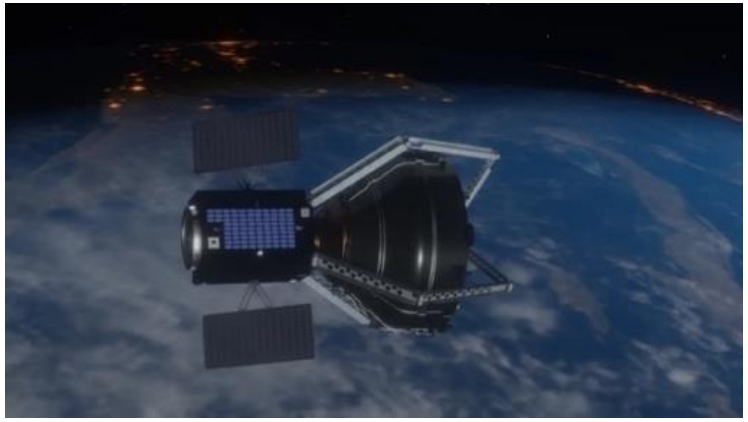

ClearSpace-1 (ESA) - 2026

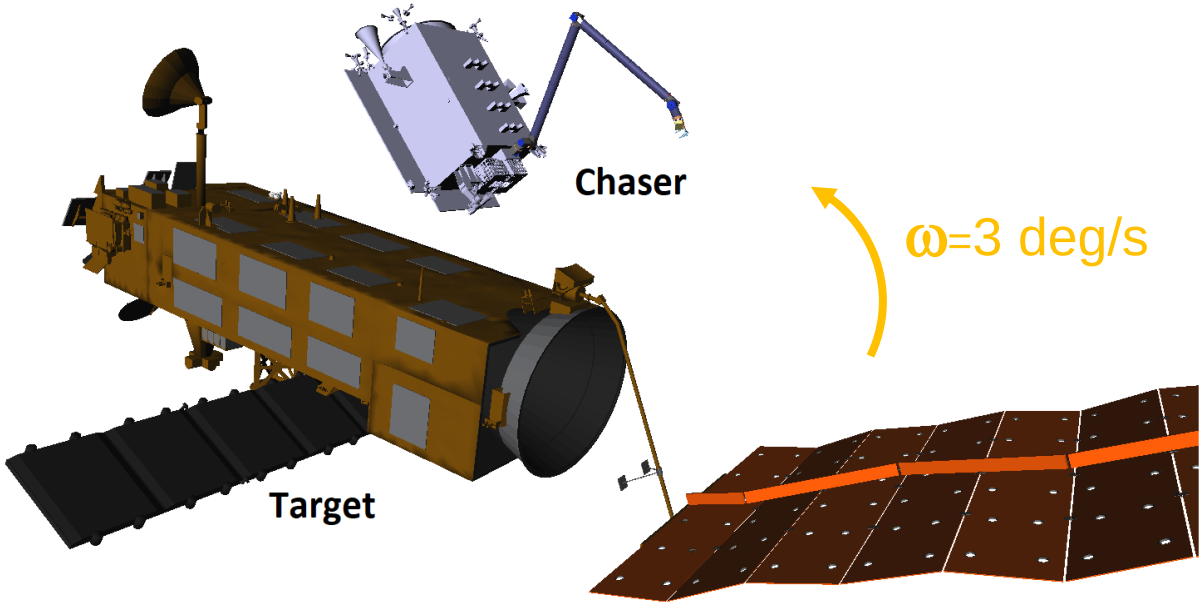

ENVISAT satellite
e.Deorbit mission study
ESA - 2016

Three Goals in Orbital Robotics

- On-orbit servicing
- Active Debris Removal
- Astronaut assistance
  - Intravehicular activities on ISS (ongoing) and future private stations
  - Dealing with cluttered, unstructured, partly unknown environments

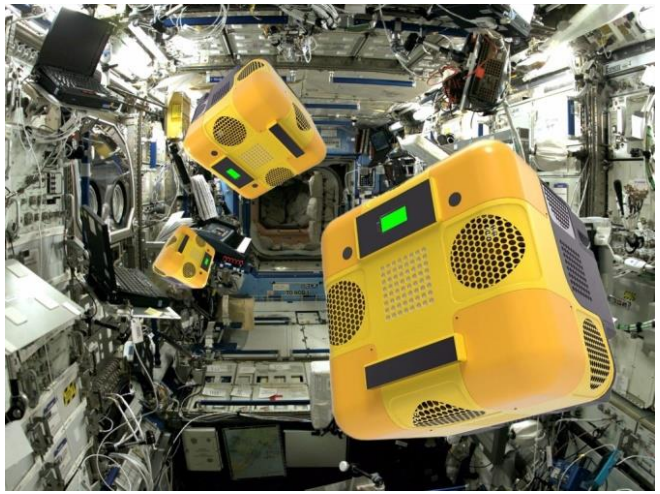

ASTROBEE on the ISS (NASA), 2020

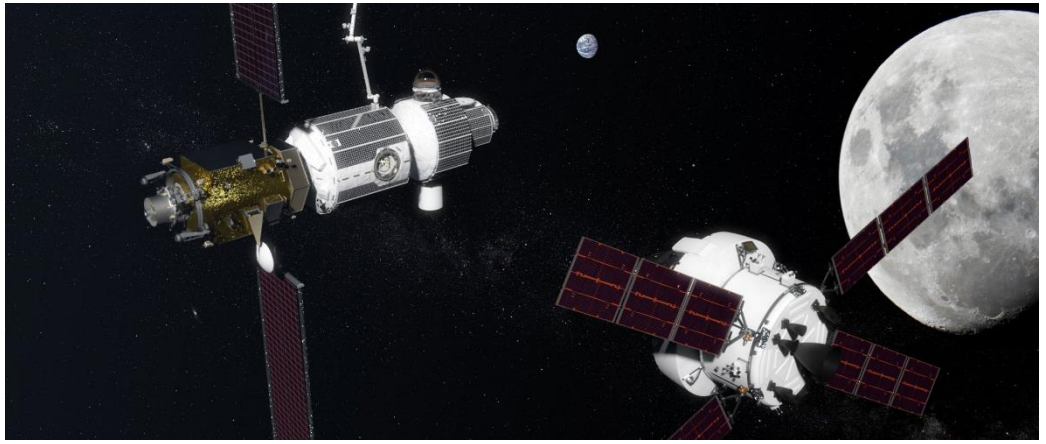

Lunar Gateway (NASA), > 2026

Project ION – Impuls Orbitale Nachhaltigkeit
DLR, 2023-25

- Research in orbital sustainability and circular economy
- Extended pipeline with debris evaluation from ground
- Methods to enhance software TRL:
  - Representative SW environment
  - Tests on OBC
  - Robustness
  - SW V&V for space

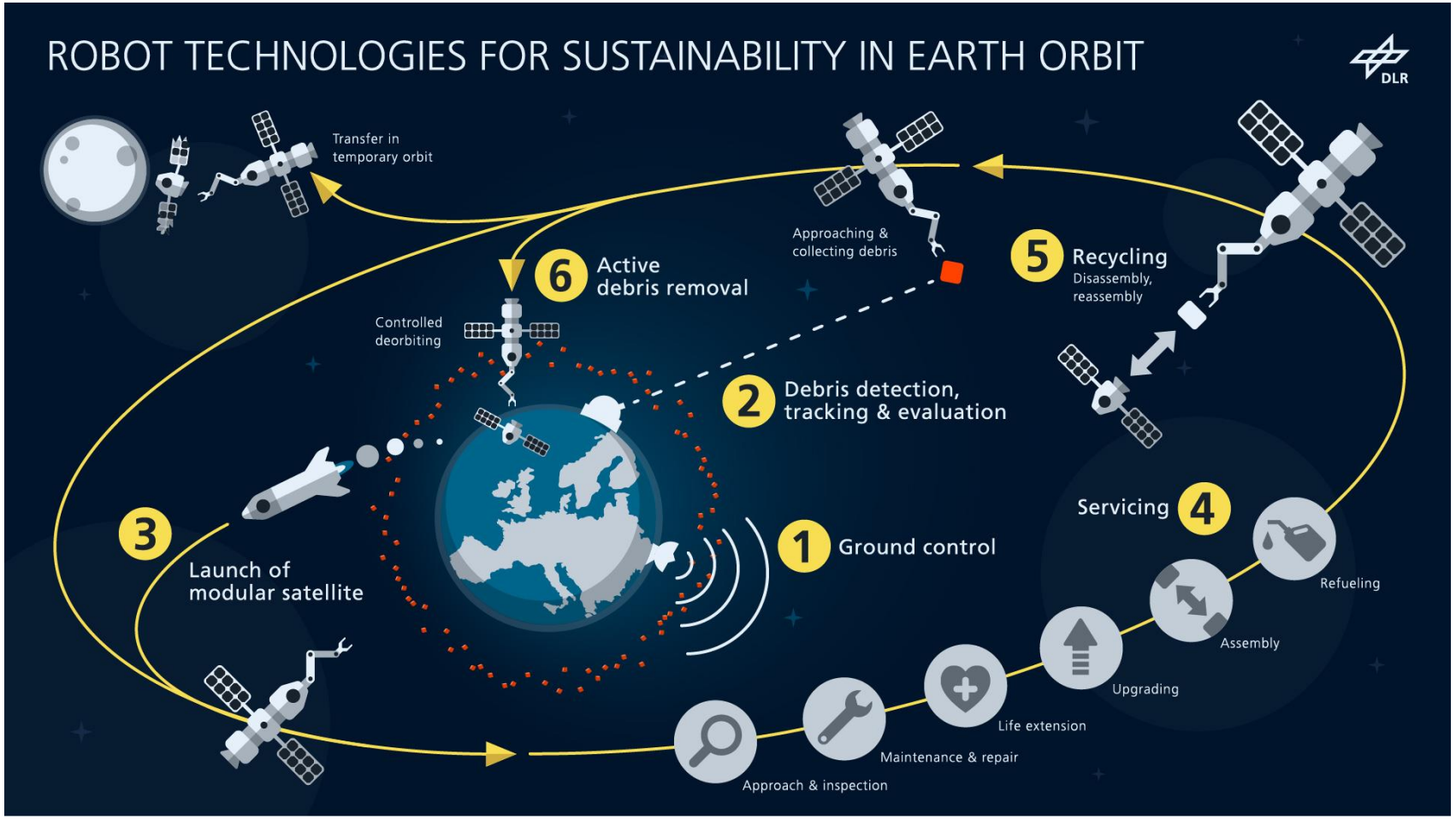

Problem statement: autonomous capture of a free-tumbling target satellite

- Vast literature on related robot control problems
  [Papadopoulos, *et al*, Frontiers in Robotics and AI, 2021]
  - Chaser rendezvous phase
  - Robot approach phase
  - Robot capture phase
  - Robot post-capture phase
- Scenarios
  - Size of target satellite
  - Geometry
  - Tumbling rate
  - …

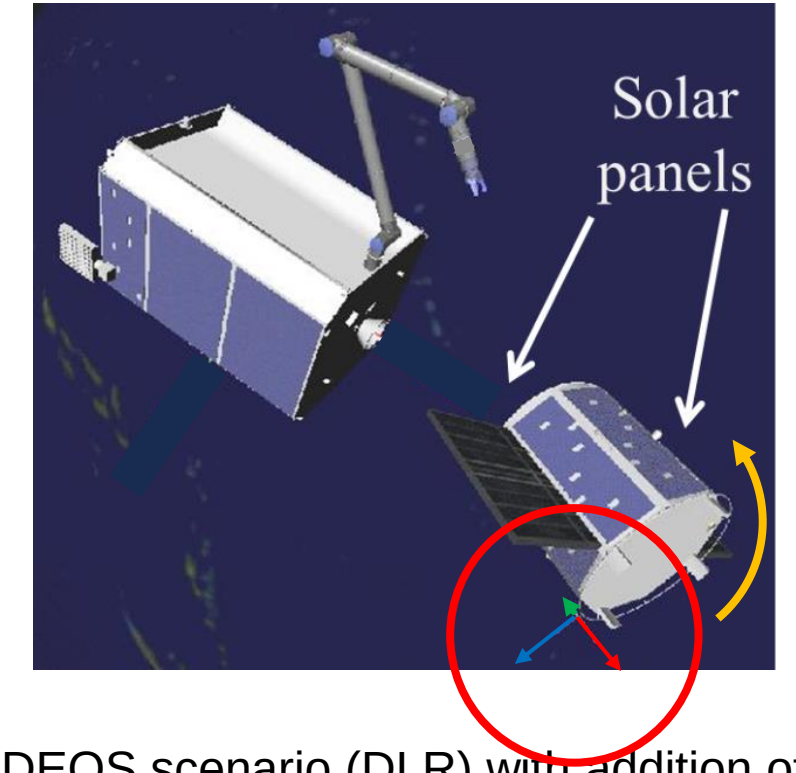

DEOS scenario (DLR) with addition of solar panels on Target

Problem statement: autonomous capture of a free-tumbling target satellite

Servicer at Observation Point in front of tumbling ENVISAT.

Servicer at Mating Point in reach of Grasping Point for capture.

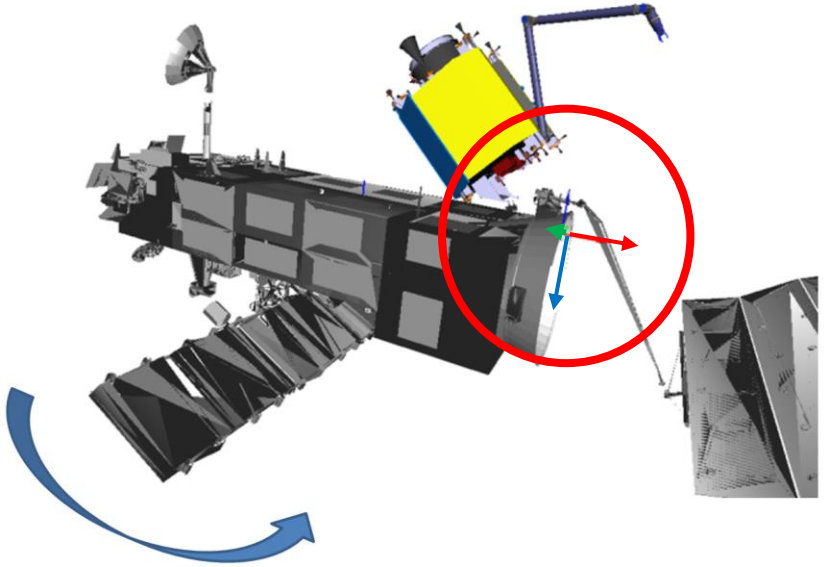

Chaser rendezvous phase

What is the typical motion of a grasping point on a tumbling target?

- Dynamics $\bar{\bar{\mathbf{I}}}.\dot{\bar{\boldsymbol{\omega}}} + \bar{\boldsymbol{\omega}} \times \bar{\bar{\mathbf{I}}}.\bar{\boldsymbol{\omega}} = \bar{\boldsymbol{\tau}} = \mathbf{0}$, initial conditions of angular velocity $\boldsymbol{\omega}$ (0) = [-2, -4, -2] deg/sec

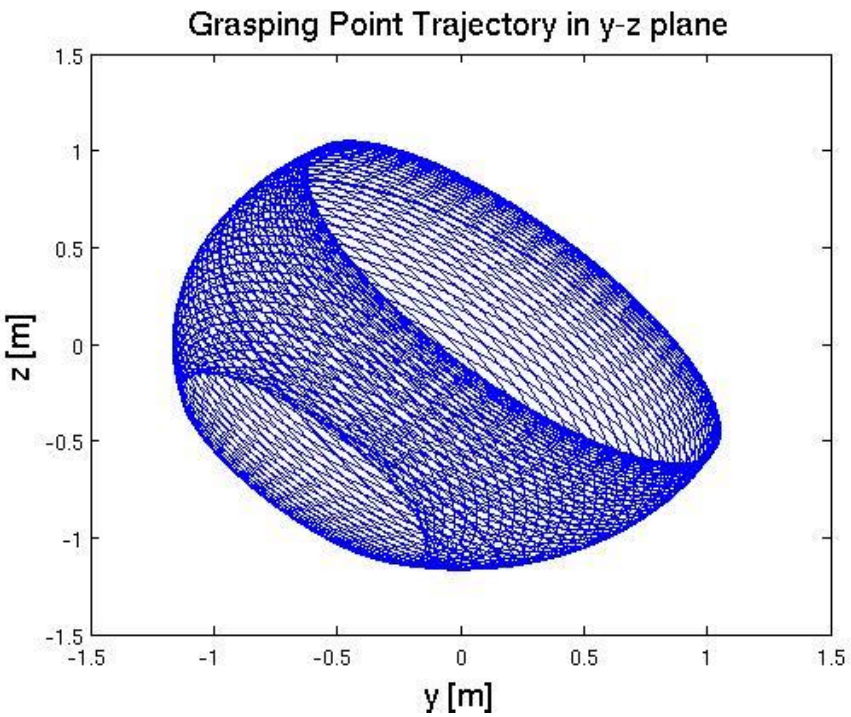

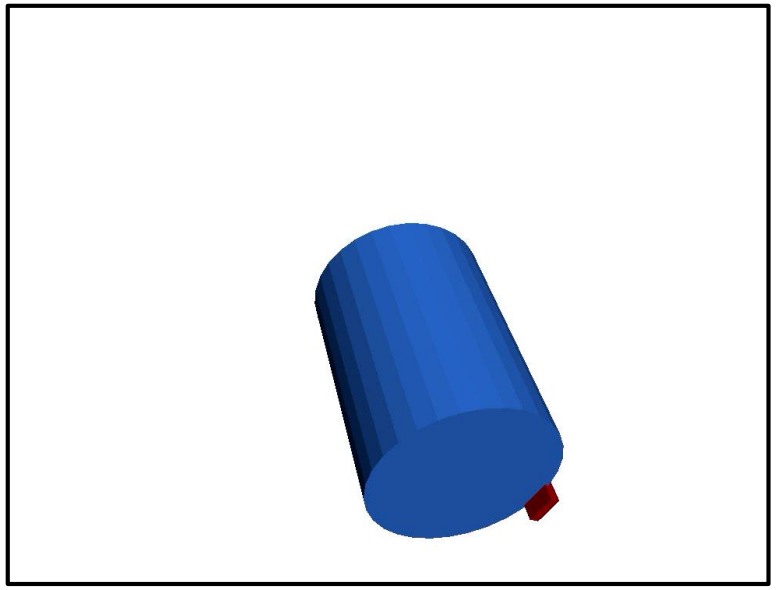

x4

Simulation time: 5000 sec (approx. 1 Low-Earth orbit)

What is the typical motion of a grasping point on a tumbling target?

- Dynamics $\bar{\bar{\mathbf{I}}}.\dot{\bar{\boldsymbol{\omega}}} + \bar{\boldsymbol{\omega}} \times \bar{\bar{\mathbf{I}}}.\bar{\boldsymbol{\omega}} = \bar{\boldsymbol{\tau}} = \mathbf{0}$, initial conditions of angular velocity $\boldsymbol{\omega}$ (0) = [-4, -2, -4] deg/sec

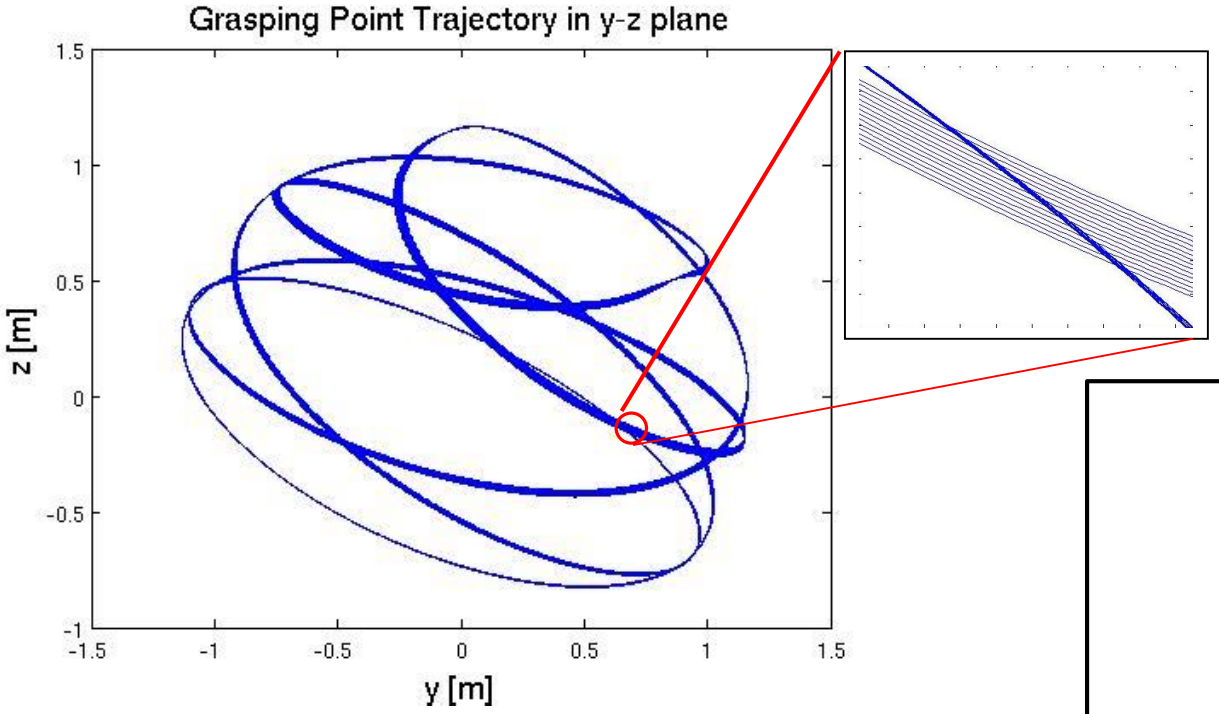

These patters are very sensitive to initial conditions and inertial properties of the body

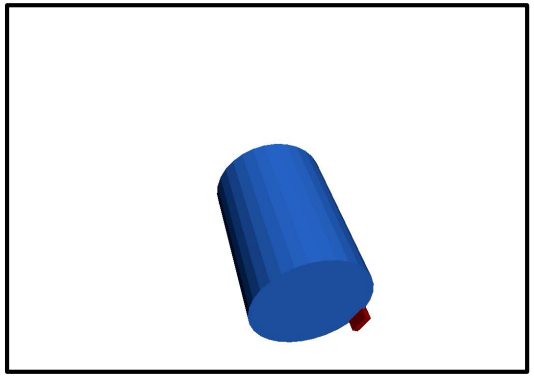

Simulation time: 5000 sec (approx. 1 Low-Earth orbit) x4

Target dynamics estimation and motion prediction – peculiarities of given problem

- Angular velocity in body frame is periodic $\boldsymbol{\omega}^{\mathrm{BF}}$

- For a rigid body in free motion, given the two motion constants
  $H^2 = \sum \mathrm{I}_i^2 \omega_i^2$ and $2T = \sum I_i\, \omega_i^2,\ I_3 < I_2 < I_1$
  and defining $D = H^2/2T$
  it can be shown that the polhode period

$$T_{\mathrm{p}} \to \infty \text{ as } D \to I_2$$

- Due to slow internal energy dissipation, a general tumble will end up in a flat spin, i.e. a pure spin about principal major axis

$$\bar{\bar{\mathbf{I}}}.\dot{\bar{\boldsymbol{\omega}}} + \bar{\boldsymbol{\omega}} \times \bar{\bar{\mathbf{I}}}.\bar{\boldsymbol{\omega}} = \boldsymbol{\tau} = c\left(\hat{\mathbf{H}}\hat{\mathbf{H}} - \bar{\bar{\mathbf{u}}}\right).\bar{\boldsymbol{\omega}}$$

Body inertia I = diag(29.2 35 38.4) kg m^2

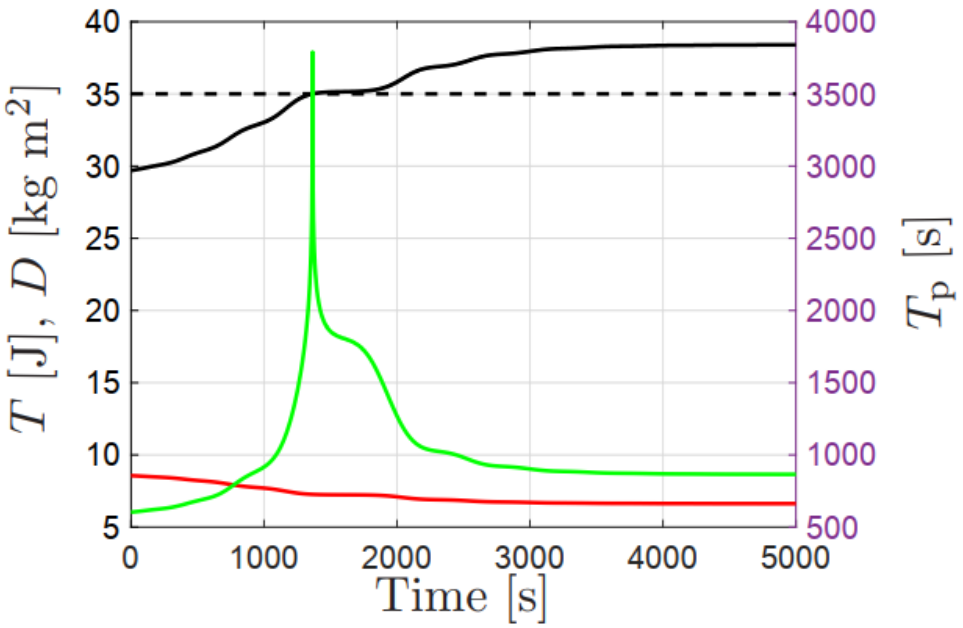

D (solid black), kinetic energy T (red) and polhode period T_{p} (green) shown during a decaying motion to a flat spin

Target dynamics estimation and motion prediction

Goal

Long-term prediction of Target motion, in the order of 60 to 600 seconds

Method

- Observe Target for time T_{obs}
- Generate pose estimates
- Identify Target inertia and state
- Predict Target motion for time T_{pred}

[Lampariello, *et al*, JGCD 2021]

Experimental pose estimates

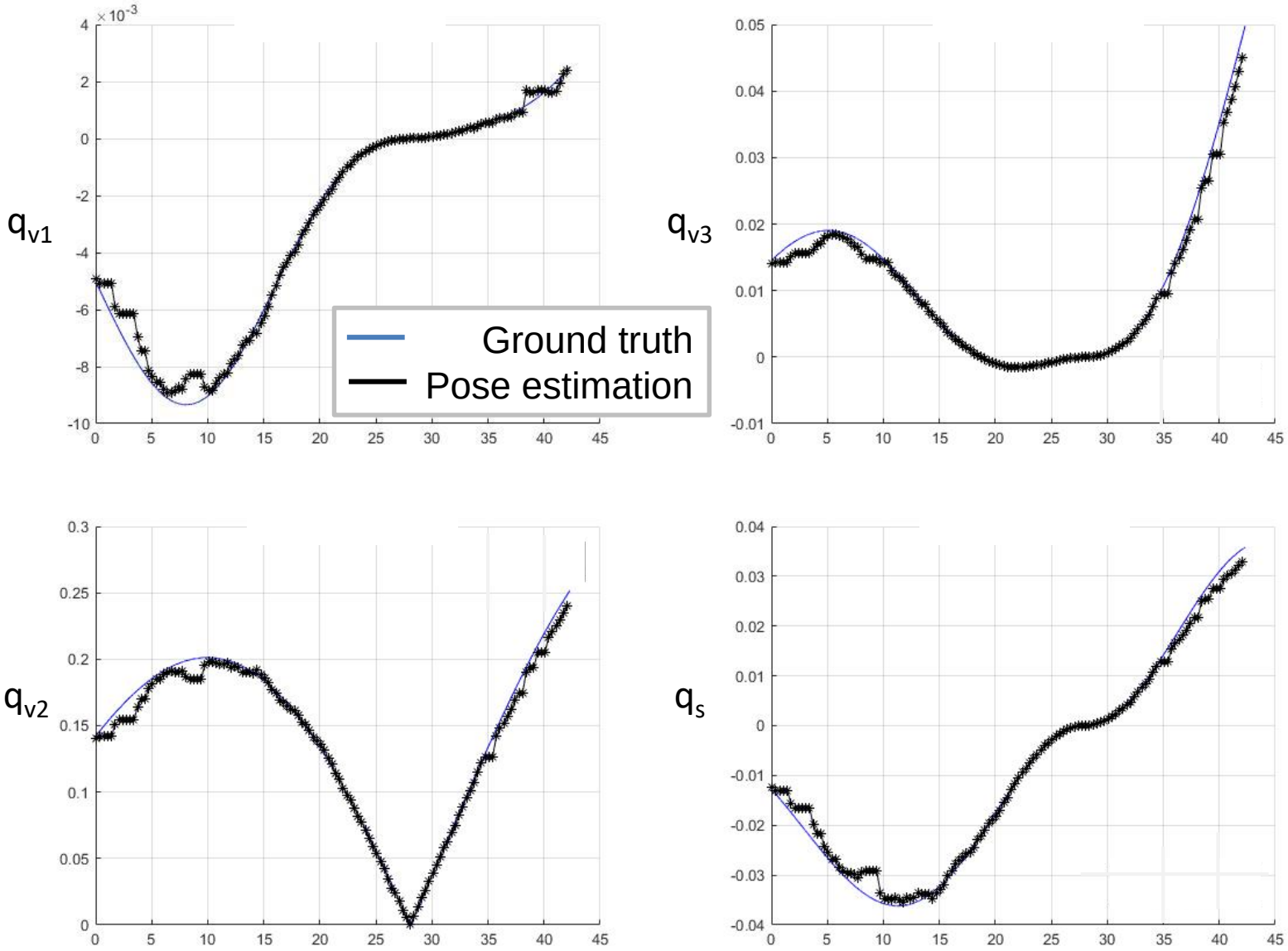

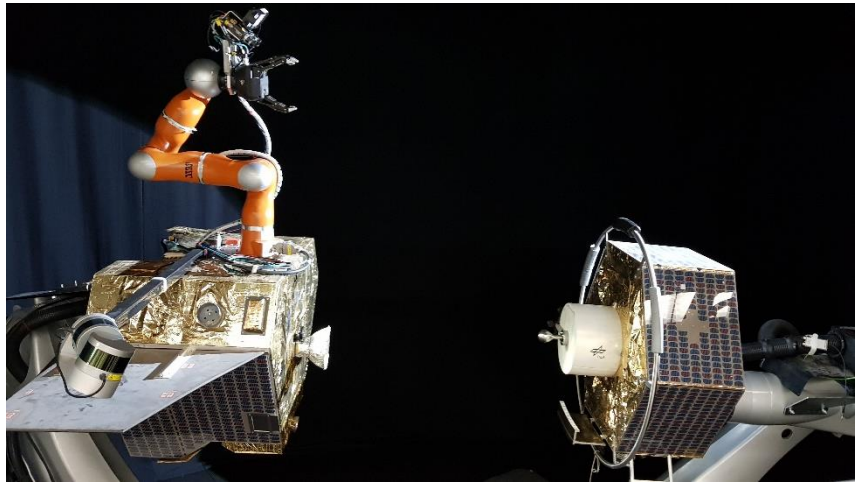

OOS-SIM facility

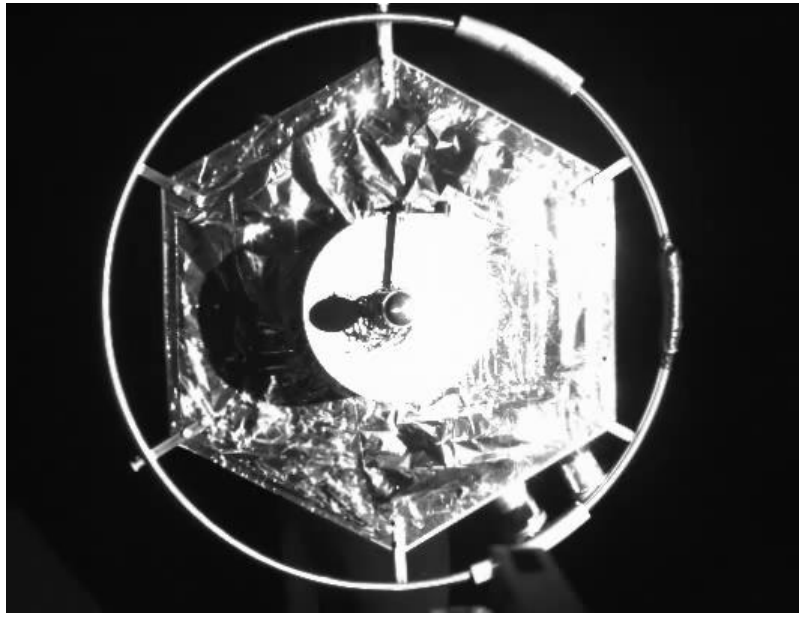

Camera image sequence

Inertia and state identification

- Nonlinear LS:

$$\left[\hat{\mathbf{I}}, \hat{\mathbf{q}}(t_0), \hat{\boldsymbol{\omega}}(t_0)\right] = \min_{[\mathbf{I}, \mathbf{q}(t_0), \boldsymbol{\omega}(t_0)]} \sum_{i=1}^{\mathrm{N}} \left\| \mathbf{q}_{\mathrm{v}}\left(t_i; \mathbf{I}, \mathbf{q}(t_0), \boldsymbol{\omega}(t_0)\right) - \widehat{\mathbf{q}_{\mathrm{v}}}(t_i) \right\|_2$$

with

$$\mathbf{q}(t) = \int_0^{\mathrm{T_{obs}}} \mathrm{C}(\mathbf{q}(t))\boldsymbol{\omega}(t)dt + \mathbf{q}(t_0) \quad \text{and} \quad \boldsymbol{\omega}(t) = \int_0^{\mathrm{T_{obs}}} \mathbf{I}^{-1}(\boldsymbol{\omega} \times \mathbf{I}\boldsymbol{\omega})dt + \boldsymbol{\omega}(t_0)$$

$$I_{ii} > 0, i \in (1,2,3) \qquad I_{ii} + I_{jj} > I_{kk}, i \neq j \neq k \in (1,2,3) \qquad \|[\hat{\mathbf{q}}(t_0), \mathbf{q}^*(t_0)]\|_2 < \delta$$

- Comparison to LS [Sheinfeld and Rock, 2009]: batch method, requires Target angular velocity
- Comparison to Extended Kalman Filter [Aghili 2009]: recursive method, assumes Gaussian noise

- Applied to five representative tumbling states of the Target, to include (close to) flat spin and perfect sphere

Motion Prediction for predefined grasping point

T_{p}=136 s, $T_{\mathrm{pred}} = 600\ s$

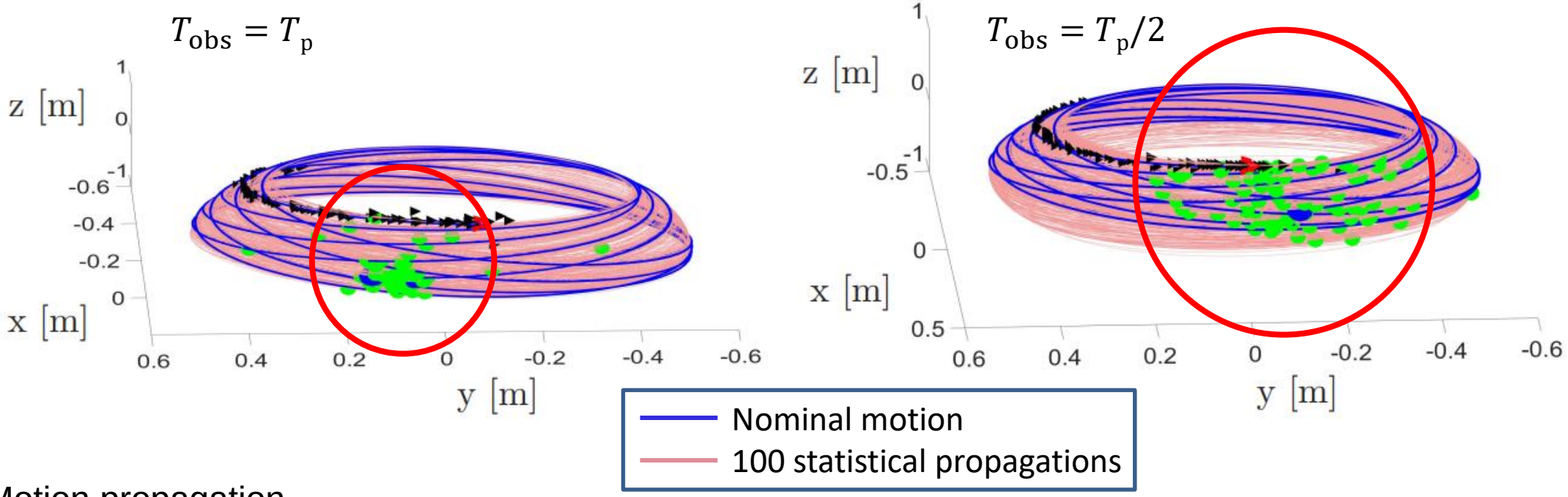

- Motion propagation
  - IVP: $\mathbf{q}(t) = \int_0^{\mathrm{T_{pred}}} \mathrm{C}(\mathbf{q}(t))\boldsymbol{\omega}(t)dt + \hat{\mathbf{q}}(t_0)$ and $\boldsymbol{\omega}(t) = \int_0^{\mathrm{T_{pred}}} \hat{\mathbf{I}}^{-1}\left(\boldsymbol{\omega} \times \hat{\mathbf{I}}\boldsymbol{\omega}\right)dt + \hat{\boldsymbol{\omega}}(t_0)$

- Dispersion characterization through propagation of Monte Carlo identification results

Optimal control-based approach

Advantages
- motion constraints
- improved performance

Application
Planetary powered landing
Spacecraft rendezvous
Planetary entry
Asteroid landing
Fuel-optimal rocket landing
Space robot trajectory planning
Attitude control
Missile guidance

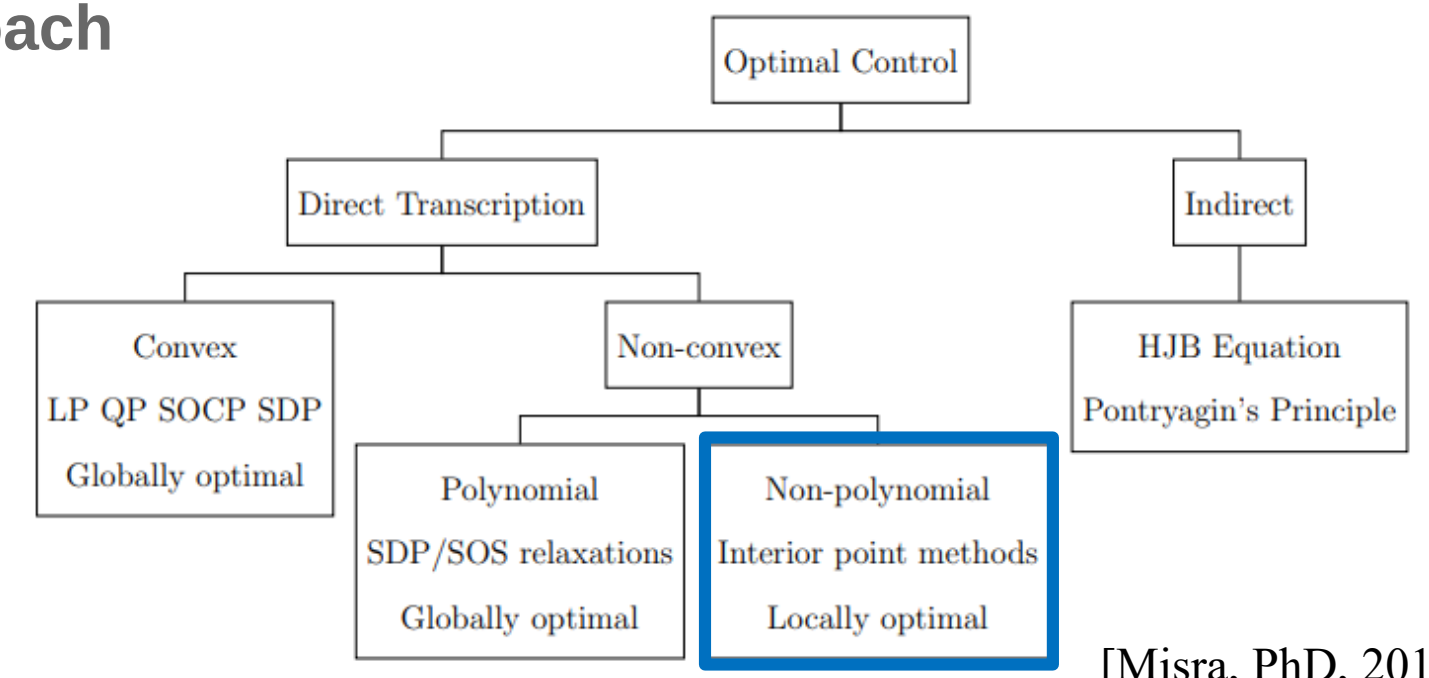

[Misra, PhD, 2019]

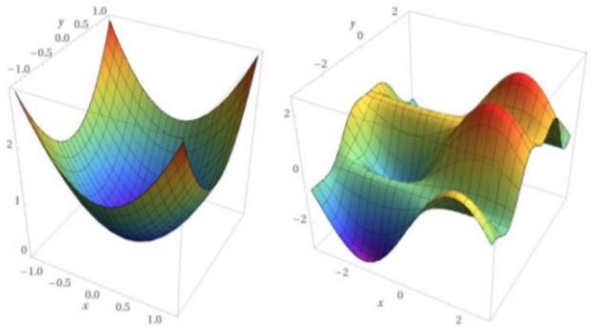

Challenges
- run-time
- convergence
- robustness
- V&V - VV4RTOS [P. Lourenco et al., ESA GNC-ICATT 2023]

Optimal control based approach – NLP formulation and resolution

$$\min_{t_f, \mathbf{q}(t), \boldsymbol{\tau}(t)} \Gamma(t_f, \mathbf{q}(t), \boldsymbol{\tau}(t))$$

$$\mathbf{g}\big(t_f, \mathbf{q}(t), \boldsymbol{\tau}(t)\big) = 0$$

$$\mathbf{h}\big(t_f, \mathbf{q}(t), \boldsymbol{\tau}(t)\big) \leq 0$$

$$0 \leq t \leq t_f$$

$$\Gamma = \int_0^{t_f} \boldsymbol{\tau}^2 \, dt \;\; \text{or} \;\; \int_0^{t_f} \left(\boldsymbol{\tau}^T \dot{\mathbf{q}}\right)^2 dt$$

$\Gamma = t_f$ [Park, 2004]

$$\Gamma = \max \min(\mathrm{TTC}(\mathbf{q}))$$

B-spline

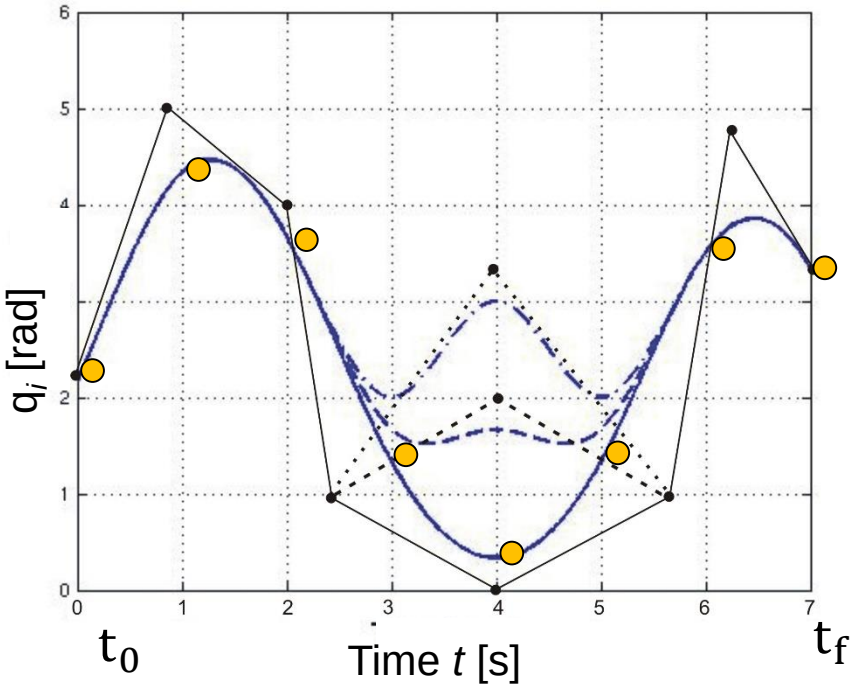

$$\mathbf{q}(t) = f(t, \mathbf{p}) \qquad \mathbf{p} \in \mathbb{R}^{N \times 1}$$

$$t_0 < t_1 < t_2 \ldots < t_{N_{via}-1} < t_f$$

Active-set
- NLOPT [Kraft, 1994]
- OCPID-DAE1 [Gerdts, 2013]

Interior Point - IPOPT

First-order
- Gusto [Bonalli, 2019]
- SCvx [Mao, 2018]

- Convexification [Liu, 2017]
- GPUs [Chretien, 2016]
- Regularization [Khadiv, Righetti, 2020]

Chaser rendezvous phase – problem statement

Compute feasible trajectory ${}^{o}\vec{\mathbf{x}}_{p}(t) \in \mathbb{R}^{6}$ to given Mating Point ⊗ and track it in view of uncertainties

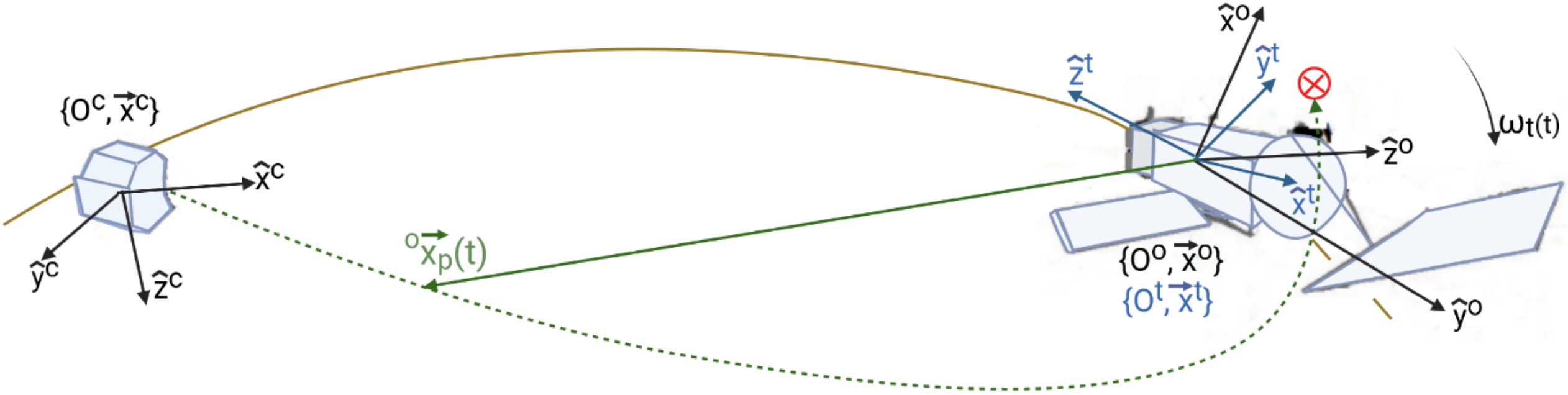

[Specht, *et al*, JGCD 2023]

Chaser rendezvous phase – optimal control

$$\min_{\mathbf{r}^0 \in \mathbb{R}^3} \Gamma = \int_0^{t_f} \left(\mathbf{F}^{0\,T}\,\dot{\mathbf{x}}^0\right)^2 \mathrm{d}t$$

$${}^{t}\mathbf{x}^{MP,C}(t_f) = {}^{t}\mathbf{x}^{MP,C}_{des}$$

$${}^{0}\ddot{x}^{0}(t) \geq 0 \quad if \quad \left\| {}^{t}\mathbf{r}^{t,0} \right\| \leq \left\| {}^{t}\mathbf{r}^{t,0} \right\|_{min}$$

$$\mathbf{PD}(t) \leq 0$$

$$\dot{\mathbf{x}}^0_{min} \leq \dot{\mathbf{x}}^0(t) \leq \dot{\mathbf{x}}^0_{max} \qquad \mathbf{F}^0_{min} \leq \mathbf{F}^0(t) \leq \mathbf{F}^0_{max}$$

– nonlinear problem
– convexification [Virgili-Llop, *et al*, IJRR, 2019]
– warm starting with LUT: $\mathbf{p} = f(\mathbf{p}_{task})$, $\mathbf{p}_{task} \in \mathbb{R}^{4\times1}$
– input from motion prediction is uncertain

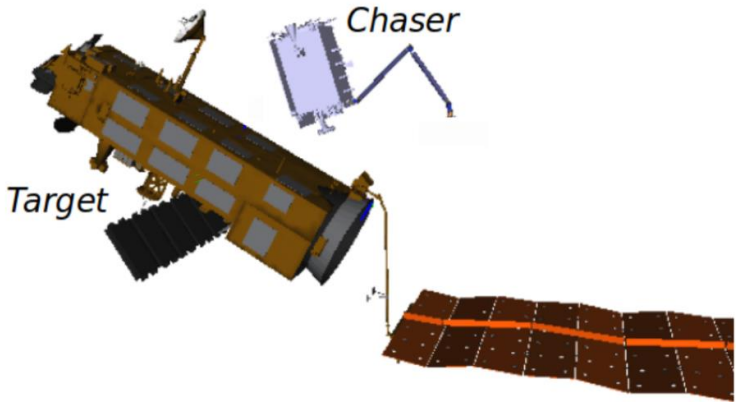

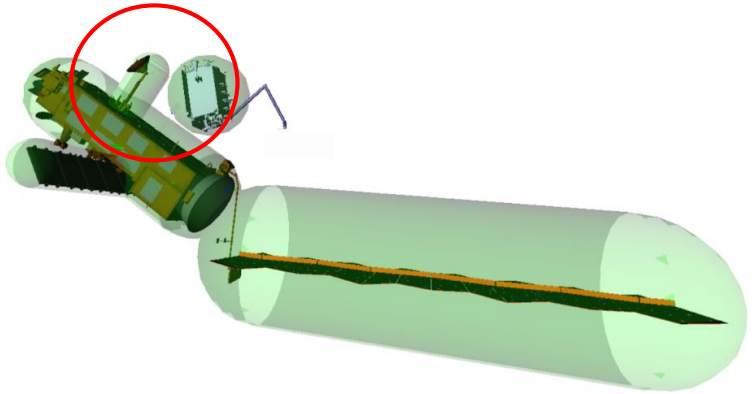

Scenario with convex hull modelling

Chaser rendezvous phase – uncertainty and tube-based MPC

Nominal case

$$ {}^{t}x_p(t) = \mathcal{R}^{to}\left(\phi_t\left(t, \omega_t(t)\right)\right) {}^{o}x_p(t) $$

Perturbed case

$$ {}^{o}x'_p(t) = \mathcal{R}^{ot}\left(\phi_t\left(t, \underline{\omega_t(t) + \delta\omega_t(t)}\right)\right) {}^{t}x_p(t) $$

Tube-based MPC:

- perturbed linear system $\dot{x}_{k+1} = \mathrm{A}x_k + \mathrm{B}u_k + w_k$
- known bounded set $w \in \mathbb{W}$
- constraints $x \in \mathbb{X}$, $u \in \mathbb{U}$

Position uncertainty ${}^{o}w_p = {}^{o}x'_p(t) - {}^{o}x_p(t)$

State uncertainty ${}^{o}w = \left[{}^{o}w_p, {}^{o}w_v\right]^T$

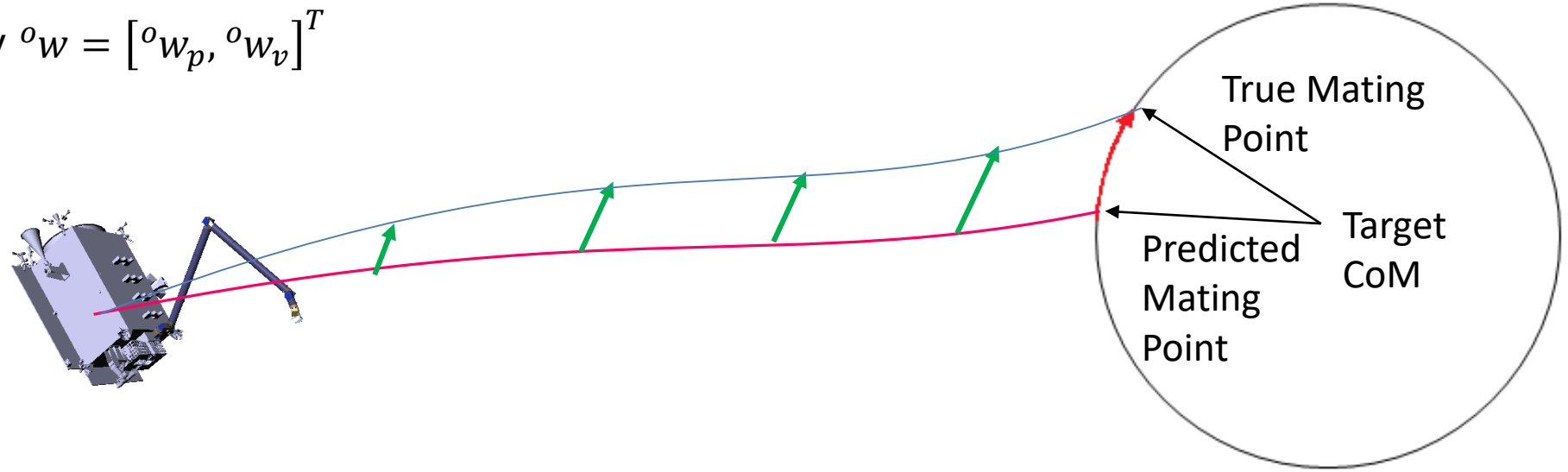

R. Lampariello, L2S, Paris, March 2024

Chaser rendezvous phase – Tube-based MPC method and solution

Solve MPC problem for nominal unperturbed system

$$\dot{z}_{k+1} = \mathrm{A}z_k + \mathrm{B}v_k$$

$$z \in \mathbb{Z},\ v \in \mathbb{V}$$

Robust control law

$$u = v + \mathrm{K}_{\mathrm{dr}}(x - z)$$

with K_{dr} - disturbance rejection gain

Uncertainty generates a tube of trajectories contained in an RPI, $\mathcal{Z}$

Constraint tightening

$$\mathbb{Z} = \mathbb{X} \ominus \mathcal{Z} \qquad \mathbb{V} = \mathbb{U} \ominus \mathrm{K}_{\mathrm{dr}}\mathcal{Z}$$

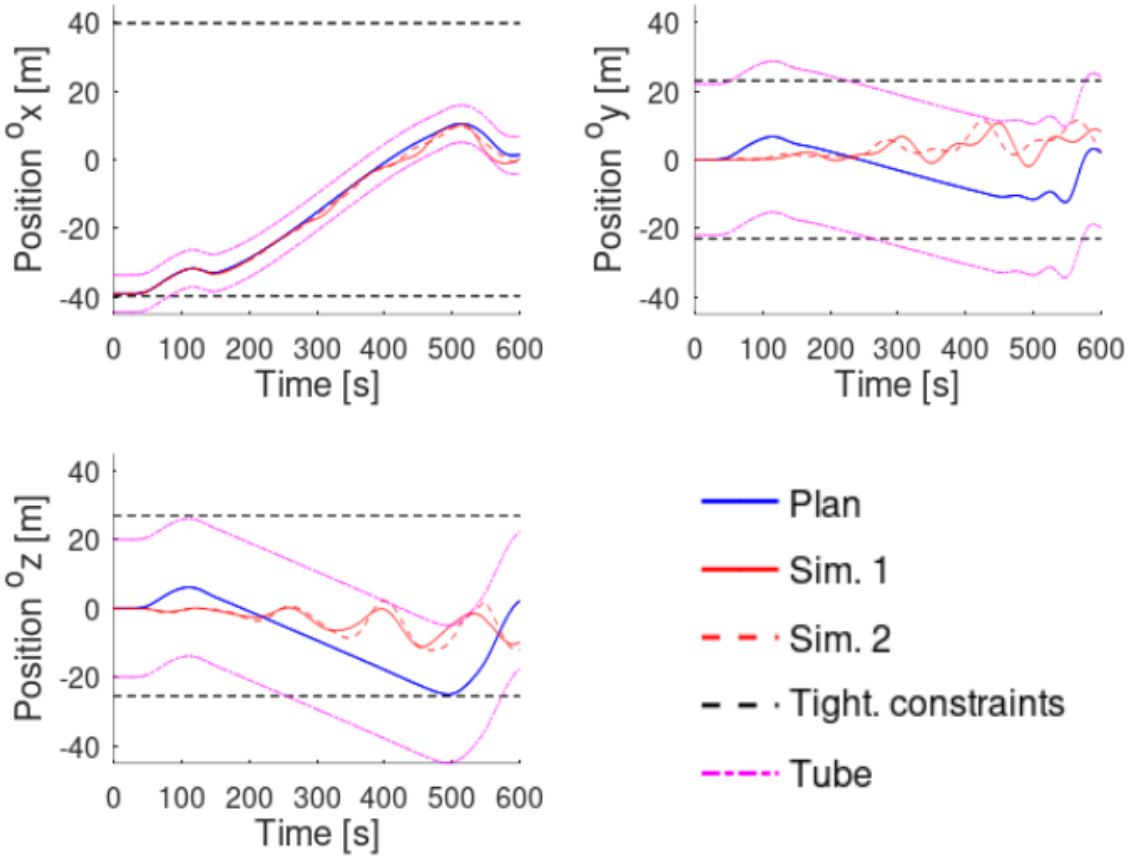

Chaser rendezvous phase – TumbleDock/ROAM Mission on ISS (DLR/MIT/NASA)

Demonstrate approach maneuvers with two ASTROBEEs

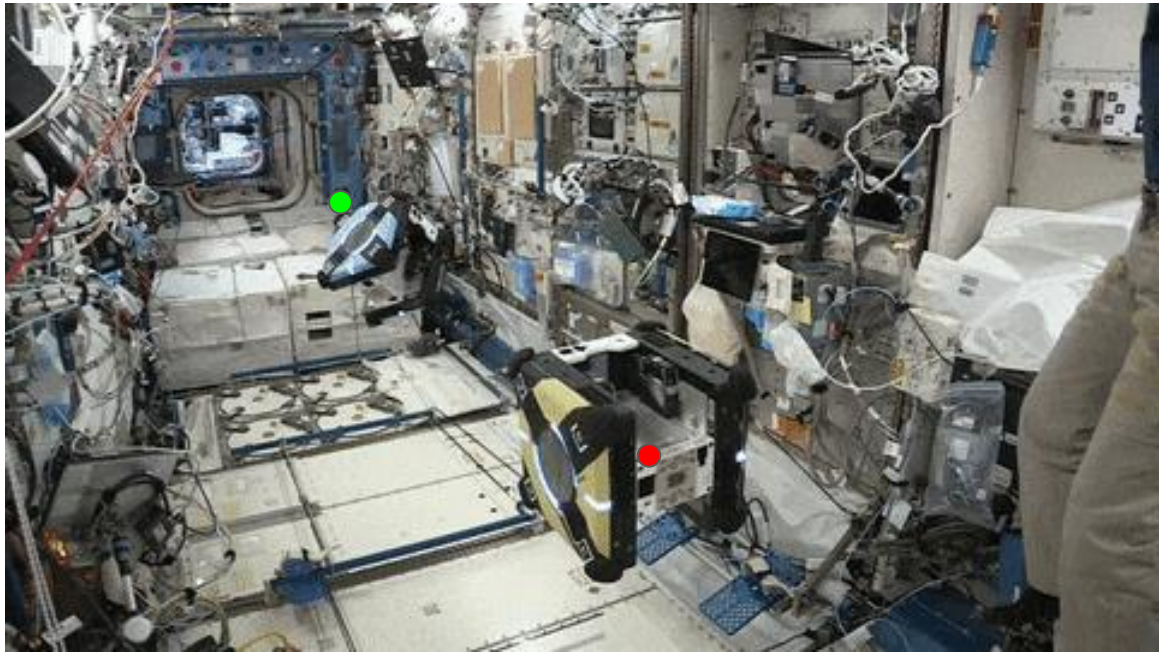

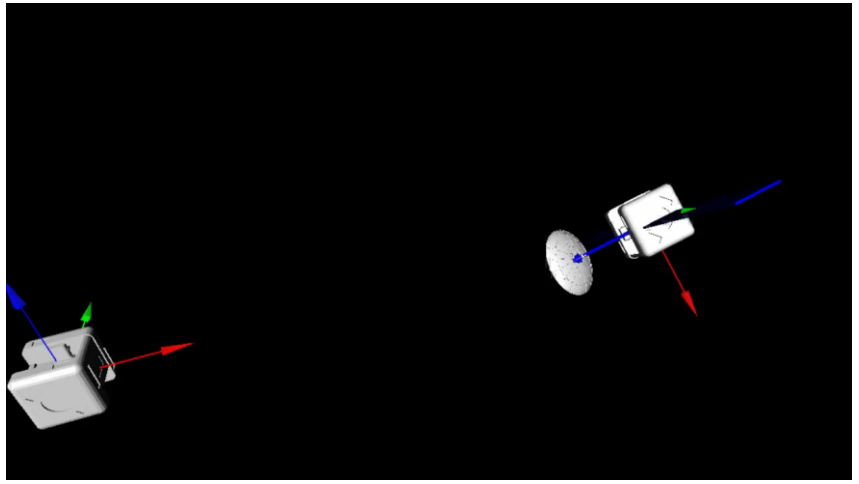

TumbleDock scenario

Albee, *et al*, Frontiers Robotics and AI, 2021
Albee, *et al*, ASTRA, 2022

TumbleDock/ROAM: Motion Planning for Rendezvous

- 13 motion planner calls,
  13 motion plans generated,
  100% motion plan generation

	Mean	Max	Min
Run time [s]	**9.16**	14.58	6.26
Chaser initial offset [m]	0.245	**0.605**	**0.004**

- Highlighted call (right):
  - ➢ Generated in 8.45 [s]
  - ➢ Chaser initial position ~0.3 [m] from expected position

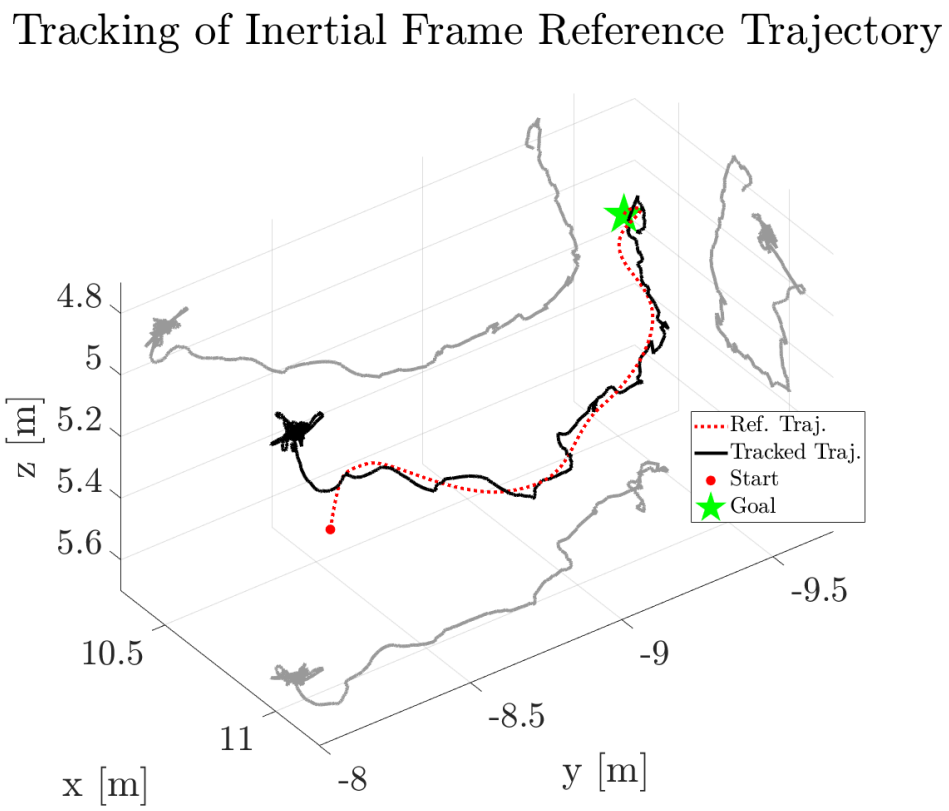

100% motion plan generation success rate

TumbleDock/ROAM: Model-Based EKF

- On-orbit validation: Closed-loop control with EKF at 62.5 [Hz]
- Successful: 19/20 runs (Target Astrobee)
- Key features:
  - ➢ Outlier rejection
  - ➢ Disturbance estimation

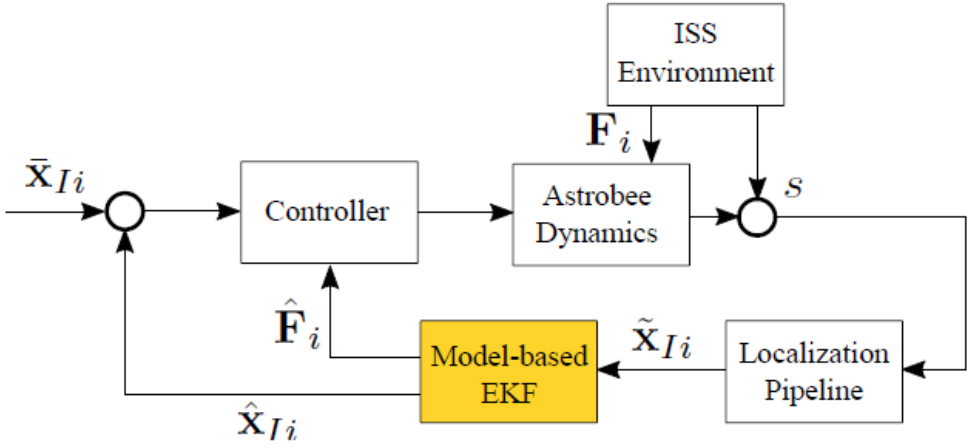

Localization discontinuities

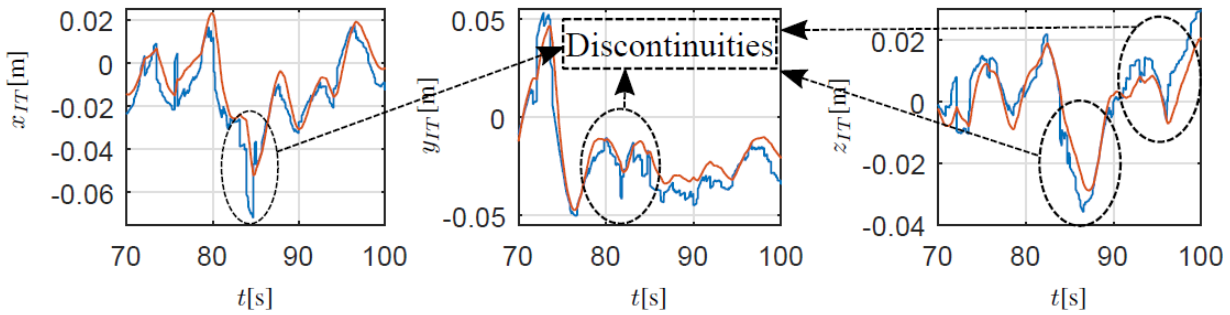

Disturbance forces

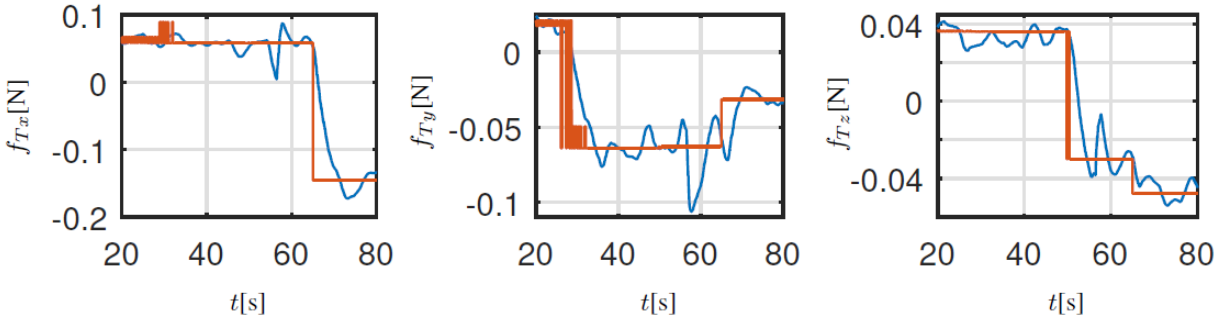

Robust and **accurate** model-based control in presence of outliers and disturbances

Free-floating Robot Dynamics

- Equations of motion

$$\begin{bmatrix} \boldsymbol{M}_b(\boldsymbol{q}) & \boldsymbol{M}_{bm}(\boldsymbol{q}) \\ \boldsymbol{M}_{bm}^{\mathrm{T}}(\boldsymbol{q}) & \boldsymbol{M}_m(\boldsymbol{q}) \end{bmatrix} \begin{bmatrix} \ddot{\boldsymbol{x}}_b \\ \ddot{\boldsymbol{q}} \end{bmatrix} + \boldsymbol{C}(\boldsymbol{q}, \dot{\boldsymbol{q}}, \dot{\boldsymbol{x}}_b) = \begin{bmatrix} \boldsymbol{0} \\ \boldsymbol{\tau} \end{bmatrix}$$

$$\dot{\boldsymbol{x}}_b \in \mathbb{R}^6,\ \boldsymbol{q} \in \mathbb{R}^{\boldsymbol{n}},\ \boldsymbol{\tau} \in \mathbb{R}^{\boldsymbol{n}}$$
$$\boldsymbol{M}_b \in \mathbb{R}^{6x6},\ \boldsymbol{M}_{bm} \in \mathbb{R}^{6\mathrm{xn}}$$

$$\mathrm{m}^{\mathrm{sys}}\dot{\mathbf{v}}^{\mathrm{CM}} = \mathbf{f}^{\mathrm{CM}}$$

$$\dot{\mathbf{L}} = \boldsymbol{\tau}^{\mathrm{CM}}$$

$$\boldsymbol{\Lambda}\ddot{\mathbf{x}}^{\mathrm{e}} + \boldsymbol{\mu}_{\mathrm{CM}}^{*} = \mathbf{F}^{\mathrm{e}} + \mathbf{J}_{\mathrm{g}}^{+\mathrm{T}}\boldsymbol{\tau} + \mathbf{J}_{\mathrm{e,CM}}^{*}\,\mathbf{F}^{\mathrm{CM}}$$

[Giordano, *et al*, 2017][Mishra, *et al*, 2023]

- Conservation of momentum, $\boldsymbol{H}$

$$\boldsymbol{M}_b\,\dot{\boldsymbol{x}}_b + \boldsymbol{M}_{bm}\dot{\boldsymbol{q}} = \boldsymbol{H} = \boldsymbol{0}$$

- Free-floating robot kinematics

$$\dot{\boldsymbol{x}}_e = \boldsymbol{J}_g(\boldsymbol{q}; \boldsymbol{M}_b, \boldsymbol{M}_{bm})\,\dot{\boldsymbol{q}}$$

- *generalized* Jacobian matrix $\boldsymbol{J}_g(\boldsymbol{q})$

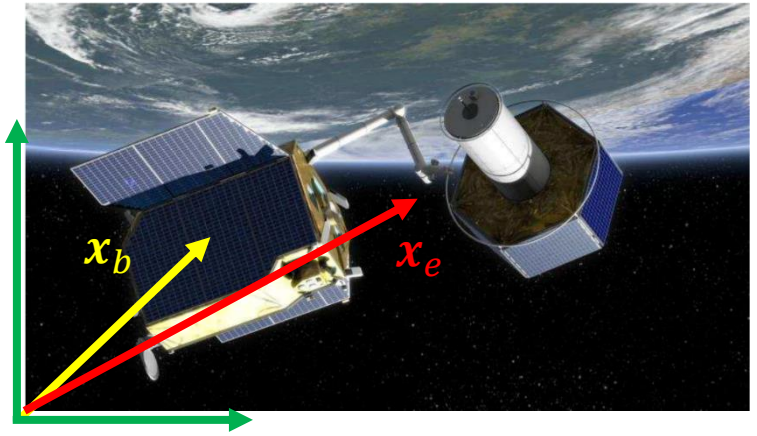

DEOS Mission Study (2015)

R. Lampariello, L2S, Paris, March 2024

Robot capture phase – approach, capture and rigidization

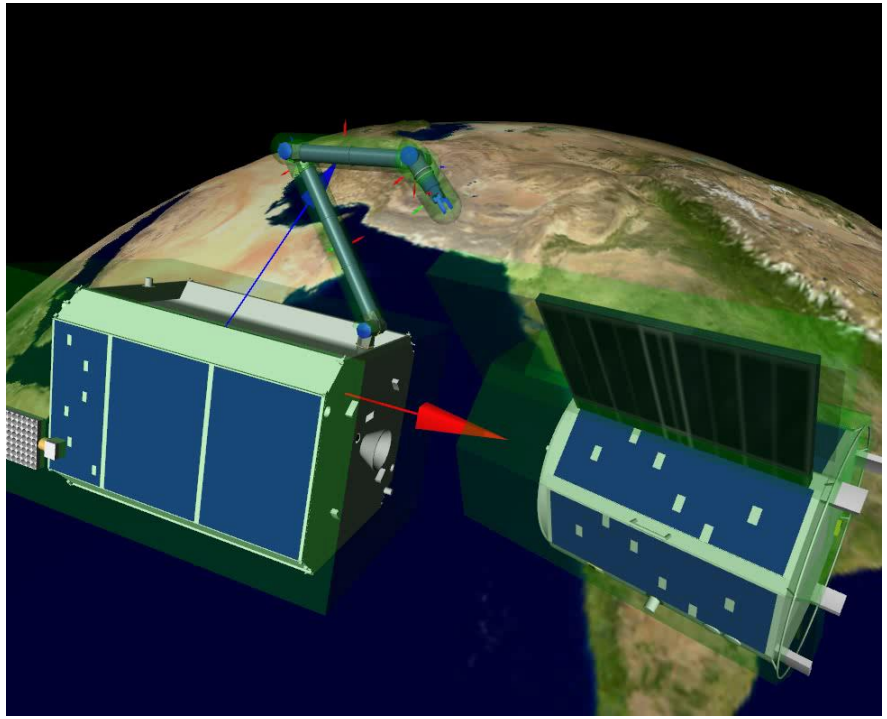

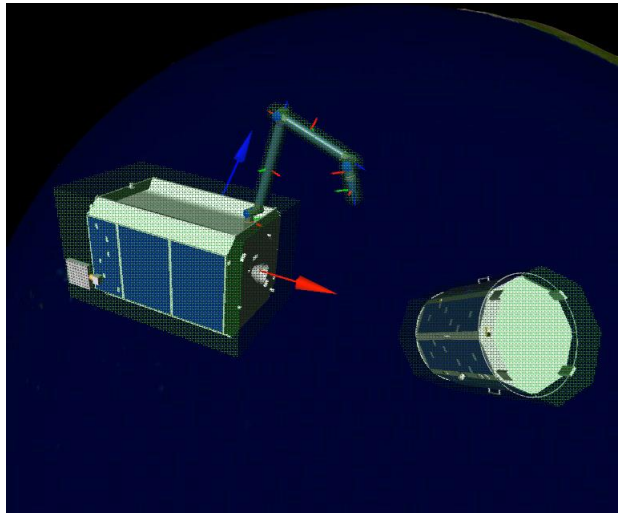

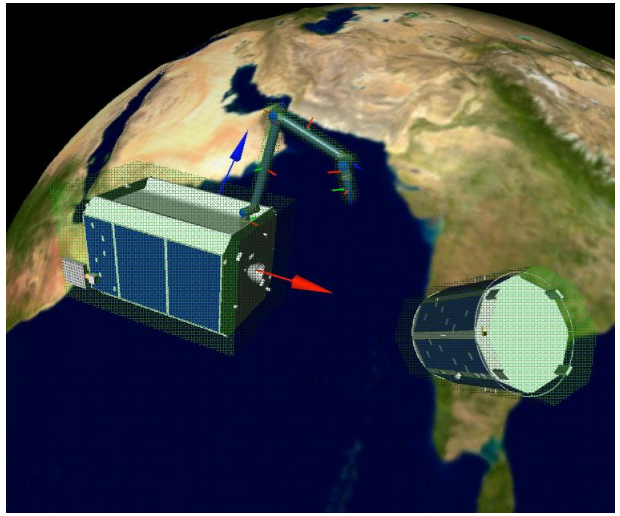

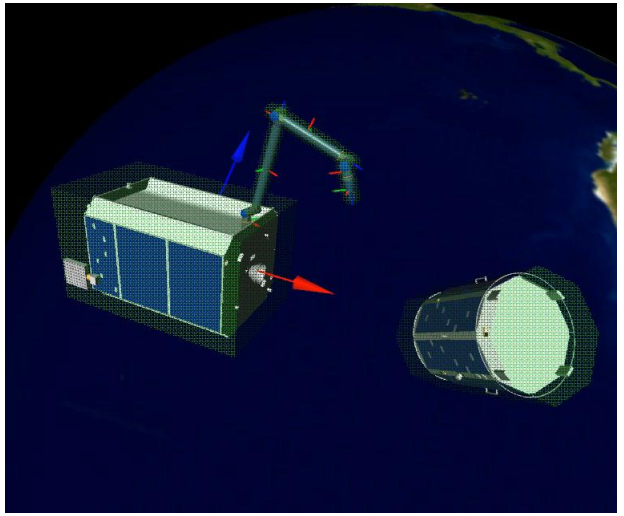

Robot capture phase

Approach NLP

$$\min_{\dot{\mathbf{q}}} \Gamma = \int_0^{t_f} \left(\boldsymbol{\tau}^T \dot{\mathbf{q}}\right)^2 dt$$

$$\mathbf{x}^e(t_f) = \int_0^{t_f} \mathbf{J}_g \, \dot{\mathbf{q}}(t) \, dt = \mathbf{x}^e_{des}$$

$$\dot{\mathbf{x}}^e(t_f) = \mathbf{J}_g \, \dot{\mathbf{q}}(t_f) = \dot{\mathbf{x}}^e_{des}$$

$$\mathbf{PD}(t) \leq 0 \qquad \mathbf{q}_{min} \leq \mathbf{q}(t) \leq \mathbf{q}_{max}$$

$$\dot{\mathbf{q}}_{min} \leq \dot{\mathbf{q}}(t) \leq \dot{\mathbf{q}}_{max} \quad \boldsymbol{\tau}_{min} \leq \boldsymbol{\tau}(t) \leq \boldsymbol{\tau}_{max}$$

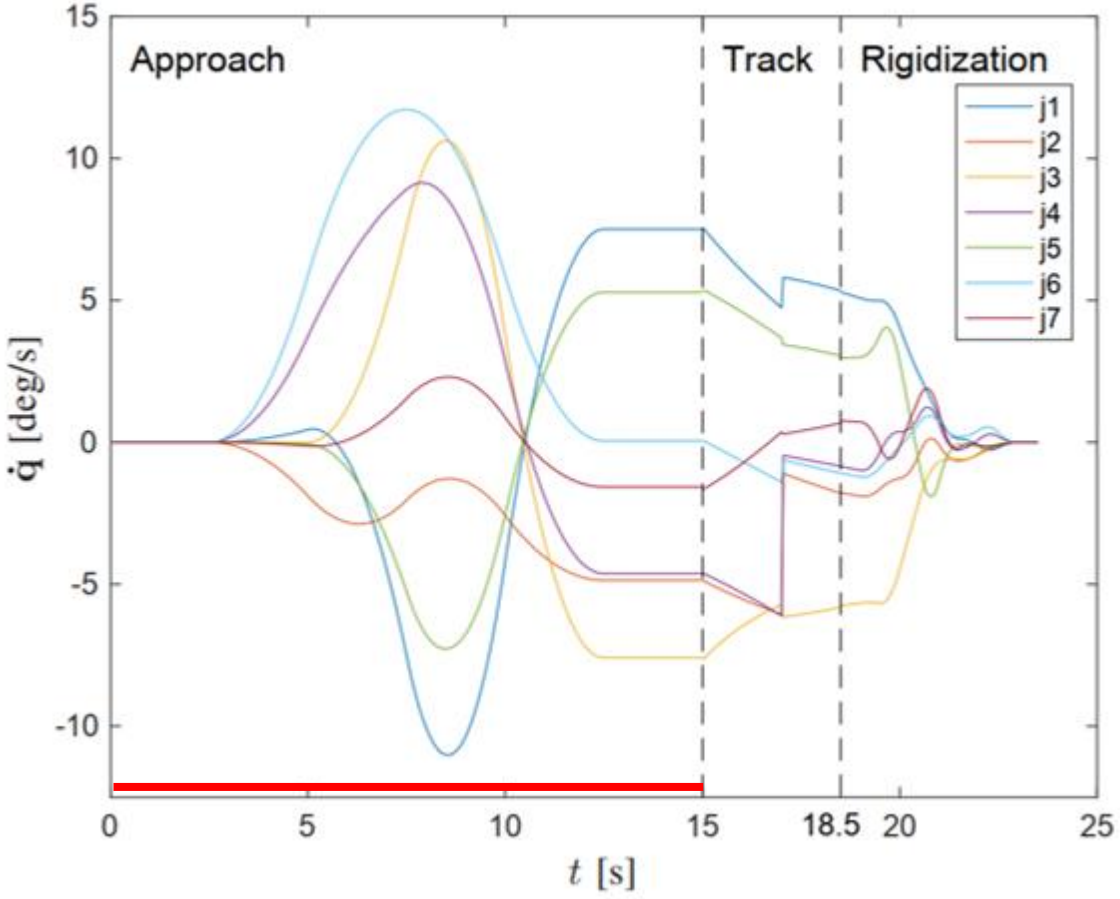

– nonlinear non-holonomic problem
– warm starting with LUT: $\mathbf{p} = f(\mathbf{p}_{task})$, $\mathbf{p}_{task} \in \mathbb{R}^{4\times1}$
– input from motion prediction is uncertain

$$\mathbf{q}(t) = f(t, \mathbf{p}) \qquad \mathbf{p} \in \mathbb{R}^{N\times1}$$

$$t_0 < t_1 < t_2 \ldots < t_{N_{via}-1} < t_f$$

[Lampariello, *et al*, IROS 2013, RA-L2018], [Virgili-Llop, *et al*, IJRR, 2019], [Agrawal, Tran. Aut. Contr., 2009]

Warm starting with Machine-Learning Regression

- Goal numerical optimization
  - Monte Carlo search for optimal solutions
  - Training set generation for discretized task space
  - Reduced problem for real-time planning
- Goal machine learning
  - Generalization via regression of input-output mapping $\mathbf{p}_{\mathrm{t}} \Rightarrow \mathbf{p}_{\mathrm{NLP}}$

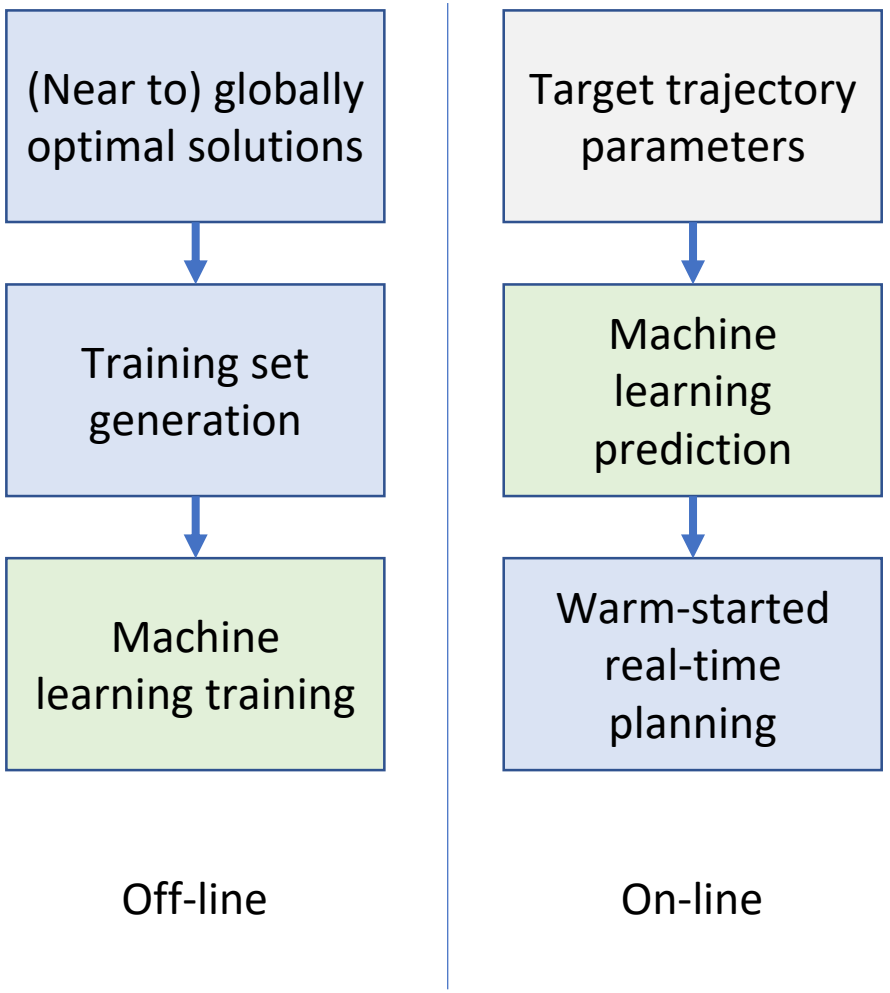

Lampariello, *et al*, ICRA 2011, ICRA 2013, 2015 [Lembono, *et al*, RAL2020], [Tenhumberg, *et al*, IROS 2022]

On-Board System Architecture for Approach and Grasping Phases

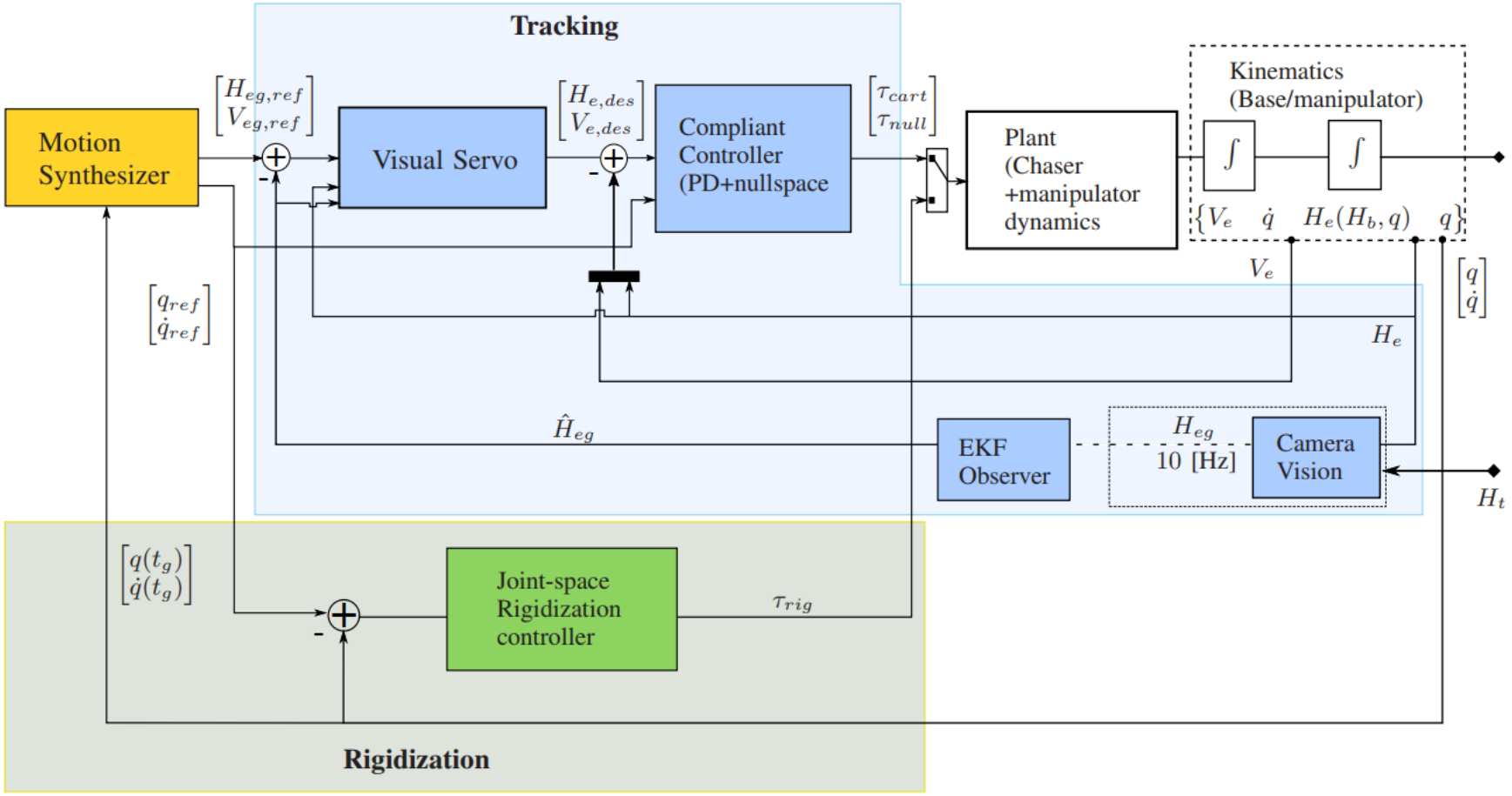

[Lampariello, *et al*, RA-L2018]

Robot capture phase – uncertainty

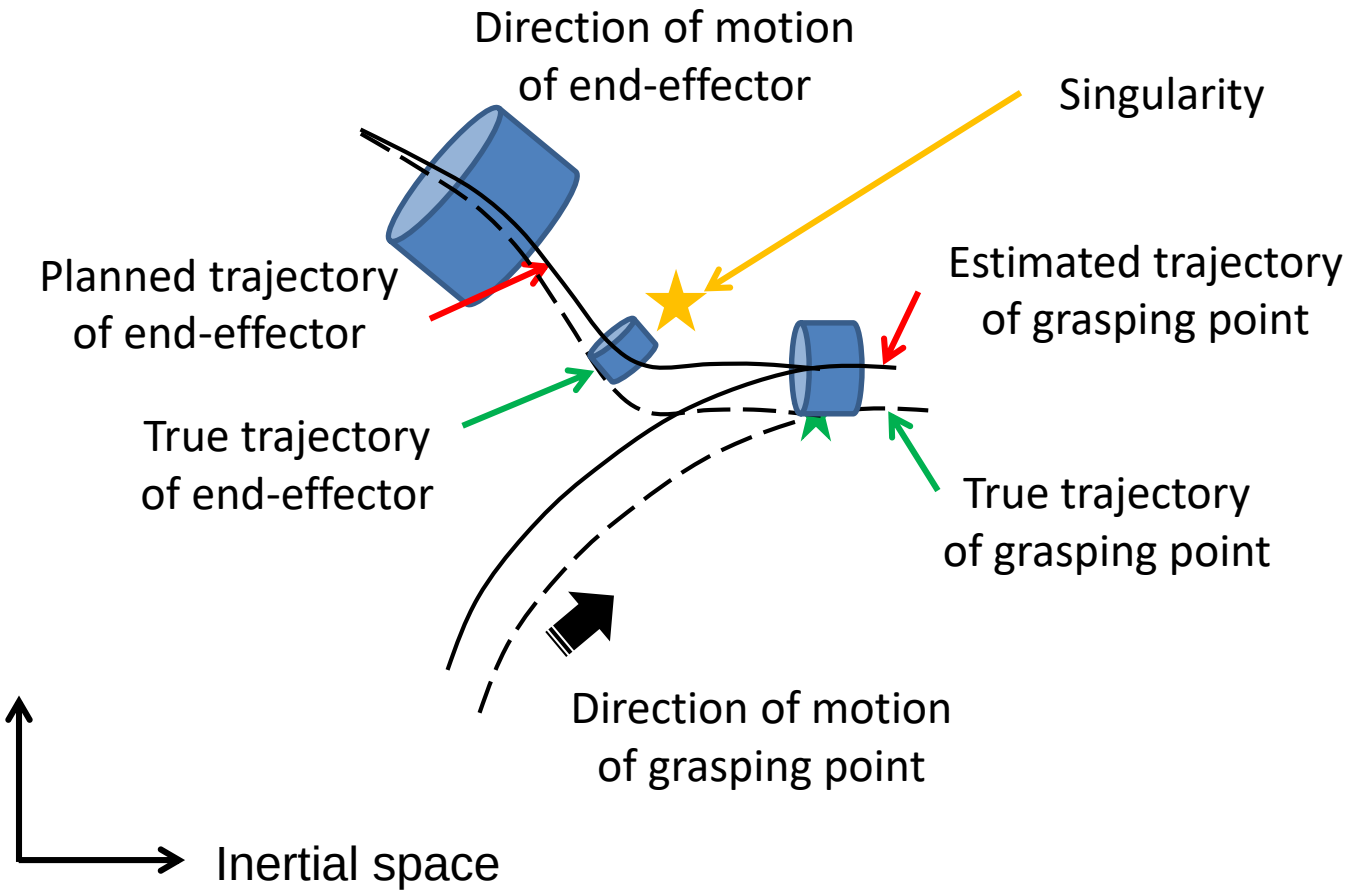

Robot capture phase – real-time control through sensitivity-based updates

Consider again a parametric NLP($\mathbf{p}_t$)

Given a nominal solution $\hat{z}(\hat{\mathbf{p}}_t)$, the Sensitivity Theorem states that
– there exists a neighborhood of validity about $\hat{\mathbf{p}}_t$
– conduct sensitivity analysis to obtain $\frac{d\hat{z}}{dp}(\hat{\mathbf{p}}_t)$

such that, for a perturbed parameter $\mathbf{p}_t \neq \hat{\mathbf{p}}_t$, compute $\bar{z}(\mathbf{p}_t)$ from Taylor approximation

$$\bar{z}(\mathbf{p}_t) = \hat{z}(\hat{\mathbf{p}}_t) + \frac{d\hat{z}}{dp}(\hat{\mathbf{p}}_t)(\mathbf{p}_t - \hat{\mathbf{p}}_t) + o(\| \mathbf{p}_t - \hat{\mathbf{p}}_t \|)$$

⟶ real-time optimal control via sensitivity analysis

[Specht, Gerdts, Lampariello, ECC 2020]

Pros
- Much reduced computational expense
- Real-time capable in most applications

Cons
- Valid locally in some Neighbourhood
- Know neighbourhood exists, but not size
- Valid within the region where the active constraint set does not change

Robot capture phase – estimate of neighborhood of validity

NLP($\mathrm{p_t}$): $$\min_{z \in \mathbb{R}^{n_z}} \quad J(z(\mathrm{p_t}), \mathrm{p_t})$$

subject to $$G_i(z(\mathrm{p_t}), \mathrm{p_t}) \leq 0, i = 1, \dots, n_G$$
$$H_j(z(\mathrm{p_t}), \mathrm{p_t}) = 0, j = 1, \dots, n_H$$

Assuming Lipschitz continuity, then

$$\|G(z(\mathrm{p_t}), \mathrm{p_t}) - G(z(\hat{\mathrm{p}}_\mathrm{t}), \hat{\mathrm{p}}_\mathrm{t})\|_q \leq L_G \|z(\mathrm{p_t}) - z(\hat{\mathrm{p}}_\mathrm{t})\|_q + L_p \|\mathrm{p_t} - \hat{\mathrm{p}}_\mathrm{t}\|_q$$

and

$$\|G(z(\mathrm{p_t}), \mathrm{p_t}) - G(z(\hat{\mathrm{p}}_\mathrm{t}), \hat{\mathrm{p}}_\mathrm{t})\|_q \leq L_G L_z \|\mathrm{p_t} - \hat{\mathrm{p}}_\mathrm{t}\|_q + L_p \|\mathrm{p_t} - \hat{\mathrm{p}}_\mathrm{t}\|_q$$

The sensitivity theorem is only valid on a consistent active constraint set, so we can derive a conservative boundary for the Neighborhood

$$G_i(z(\mathrm{p_t}), \mathrm{p_t}) \leq G_i(z(\hat{\mathrm{p}}_\mathrm{t}), \hat{\mathrm{p}}_\mathrm{t}) + \left(L_G L_z + L_p\right)\|\mathrm{p_t} - \hat{\mathrm{p}}_\mathrm{t}\|_q \overset{!}{\leq} 0, \qquad i \notin A(\hat{z}(\hat{\mathrm{p}}_\mathrm{t}), \hat{\mathrm{p}}_\mathrm{t})$$

- active constraint set

or

$$\|\mathrm{p_t} - \hat{\mathrm{p}}_\mathrm{t}\|_q \leq \frac{1}{L_G L_z + L_p} \min_{i \notin A(\hat{z}(\hat{\mathrm{p}}_\mathrm{t}), \hat{\mathrm{p}}_\mathrm{t})} \{-G_i(z(\hat{\mathrm{p}}_\mathrm{t}), \hat{\mathrm{p}}_\mathrm{t})\}$$

- L_G, L_z and L_p estimated from sensitivity analysis

Robot capture phase – neighborhood of validity for 2D example

Example: two-link planar arm, point-to-point motion

Parameter $\mathrm{p_t} = q(t_f) = [q^1, q^2]$

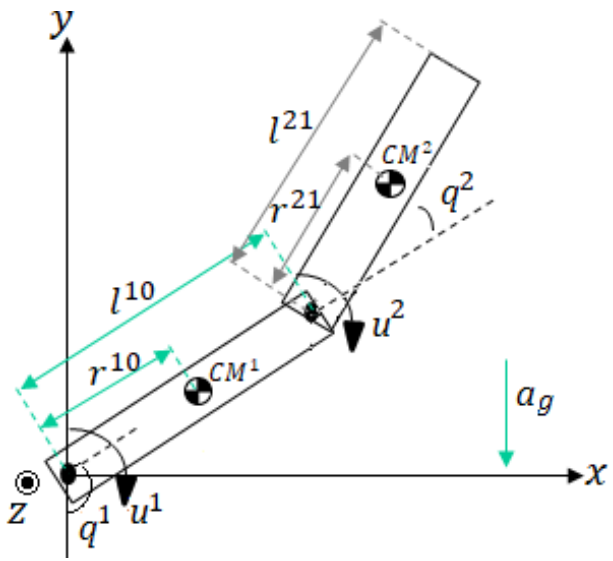

Model

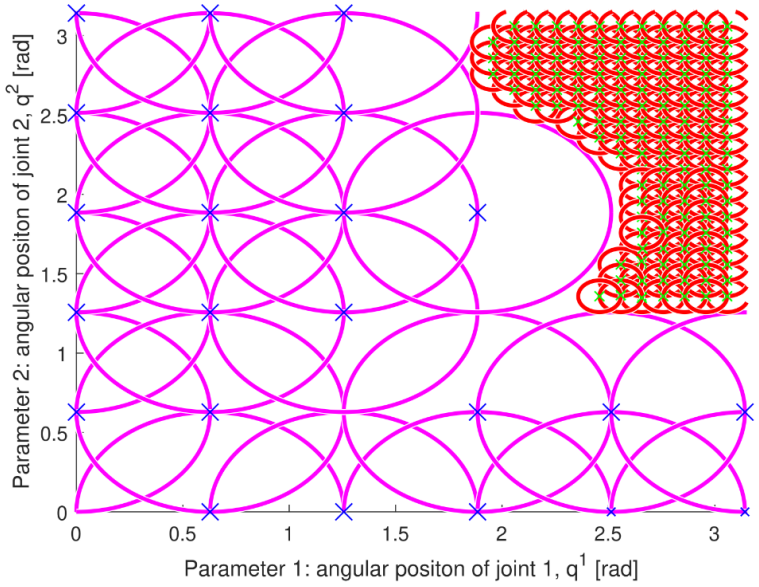

Two active set groups

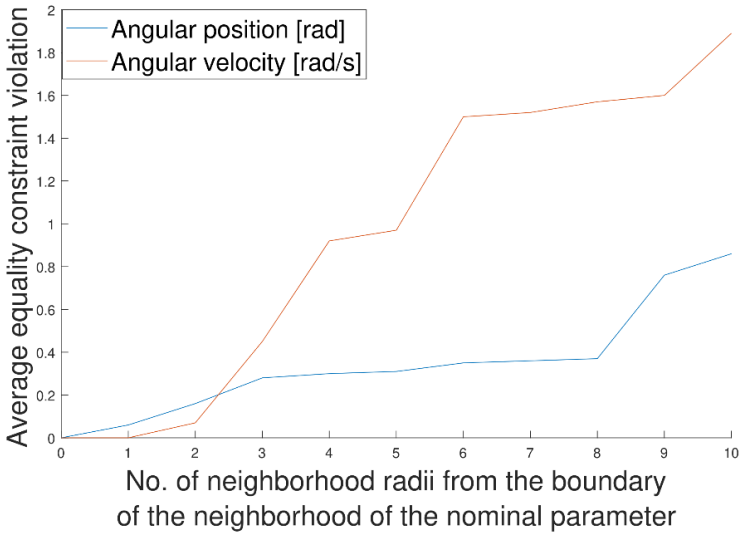

Performance analysis

Robot capture phase

Tracking NLP

$$\dot{\mathbf{q}}(t) = \mathbf{J}_{\mathrm{g}}^{-1}\, \dot{\mathbf{x}}_{\mathrm{des}}^{\mathrm{e}}(t)$$

$$\mathbf{q}(t) = \int_0^t \mathbf{J}_{\mathrm{g}}^{-1}\, \dot{\mathbf{x}}_{\mathrm{des}}^{\mathrm{e}}(t)\, \mathrm{dt}$$

$$\mathbf{PD}(t) \leq 0 \qquad \mathbf{q}_{\min} \leq \mathbf{q}(t) \leq \mathbf{q}_{\max}$$

$$\dot{\mathbf{q}}_{\min} \leq \dot{\mathbf{q}}(t) \leq \dot{\mathbf{q}}_{\max} \quad \boldsymbol{\tau}_{\min} \leq \boldsymbol{\tau}(t) \leq \boldsymbol{\tau}_{\max}$$

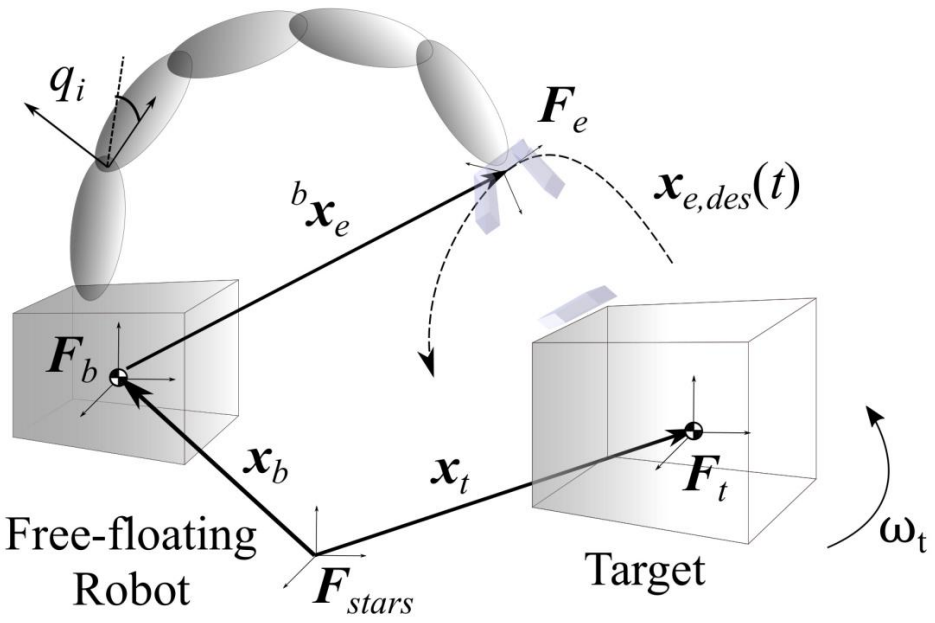

– Jacobian inverse $\mathbf{J}_{\mathrm{g}}^{-1}$

Singularity Map of a Free-floating Robot

$$\dot{\mathbf{q}}(t) = \mathbf{J}_{\mathrm{g}}^{-1}(\mathbf{q}; \mathbf{M}_{\mathrm{b}}, \mathbf{M}_{\mathrm{bm}})\, \dot{\mathbf{x}}_{\mathrm{des}}^{\mathrm{e}}(t)$$

- Dynamic Singularities [Papadopoulos, 1993]
  - Path dependent
  - Independent of last robot arm joint position
- Generation of a singularity map in robot joint space with Interval Arithmetic or Taylor Models
  - Completeness
  - Lipchitz continuity

[Calzolari, Lampariello, Giordano, RSS 2020]

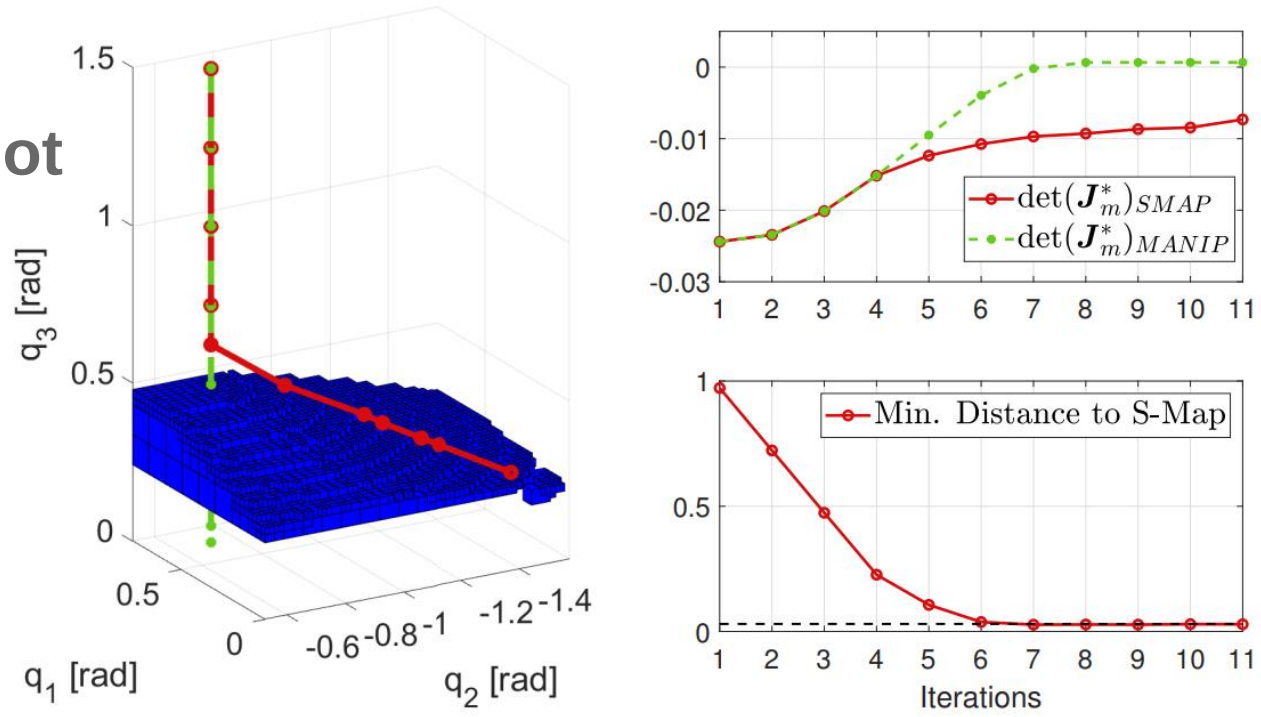

Singularity map within gradient-based trajectory optimization

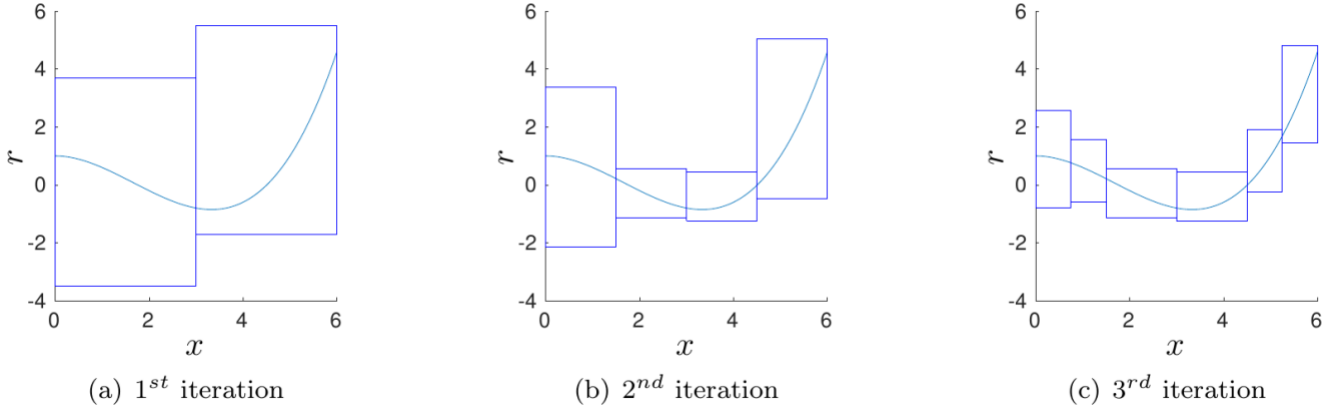

(a) 1st iteration (b) 2nd iteration (c) 3rd iteration

Recursive Branch and Bound for Taylor Models [Althoff, 2018]

EROSS IOD (EU, 2021-24)

Concept

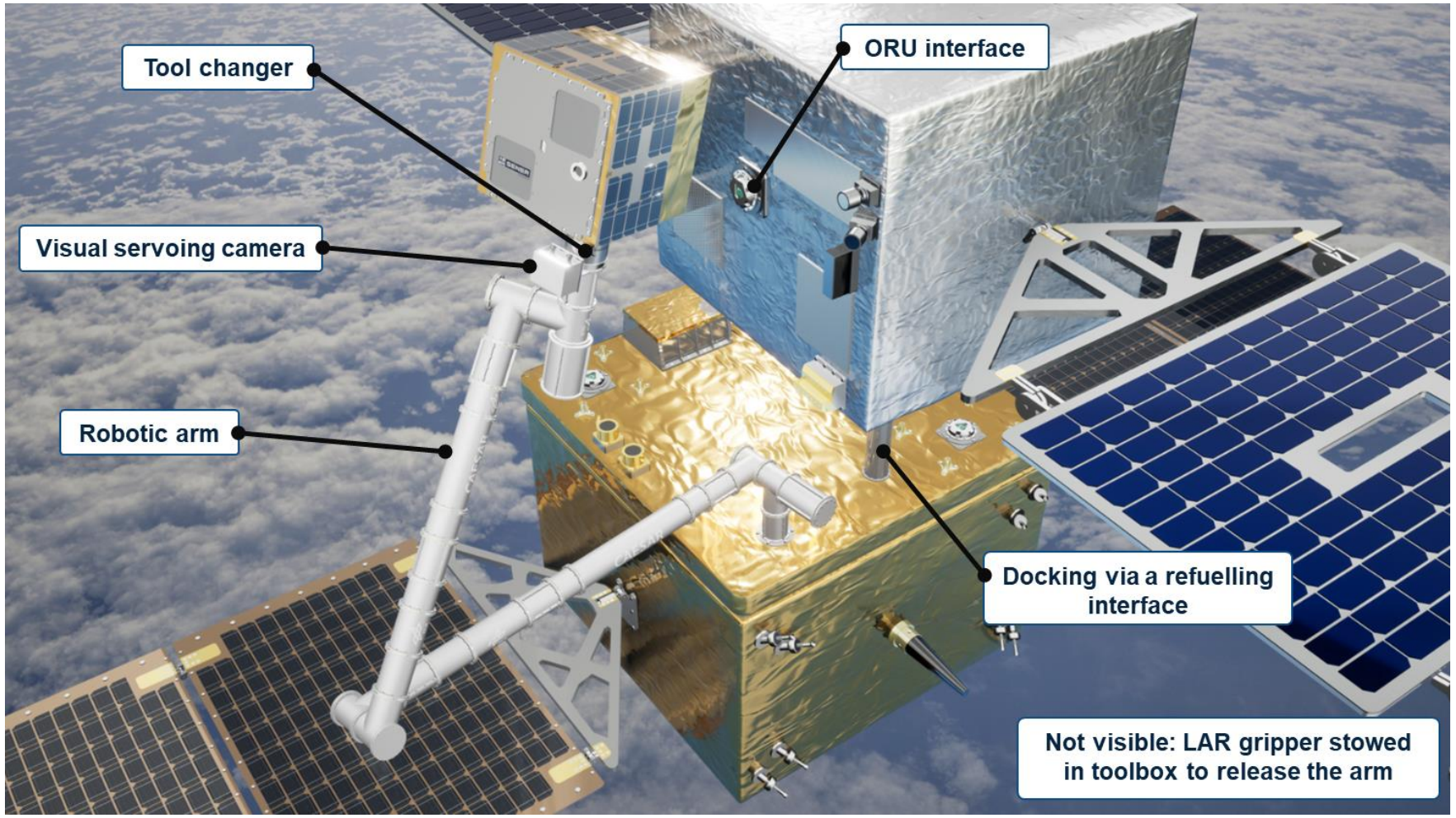

Past and On-going Activities for ADR

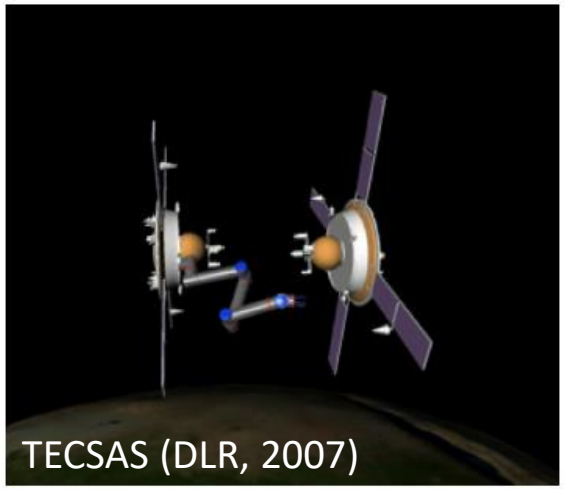
TECSAS (DLR, 2007)

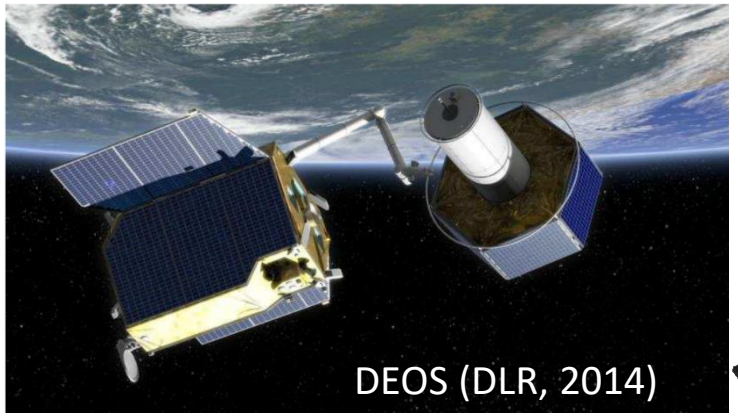
DEOS (DLR, 2014)

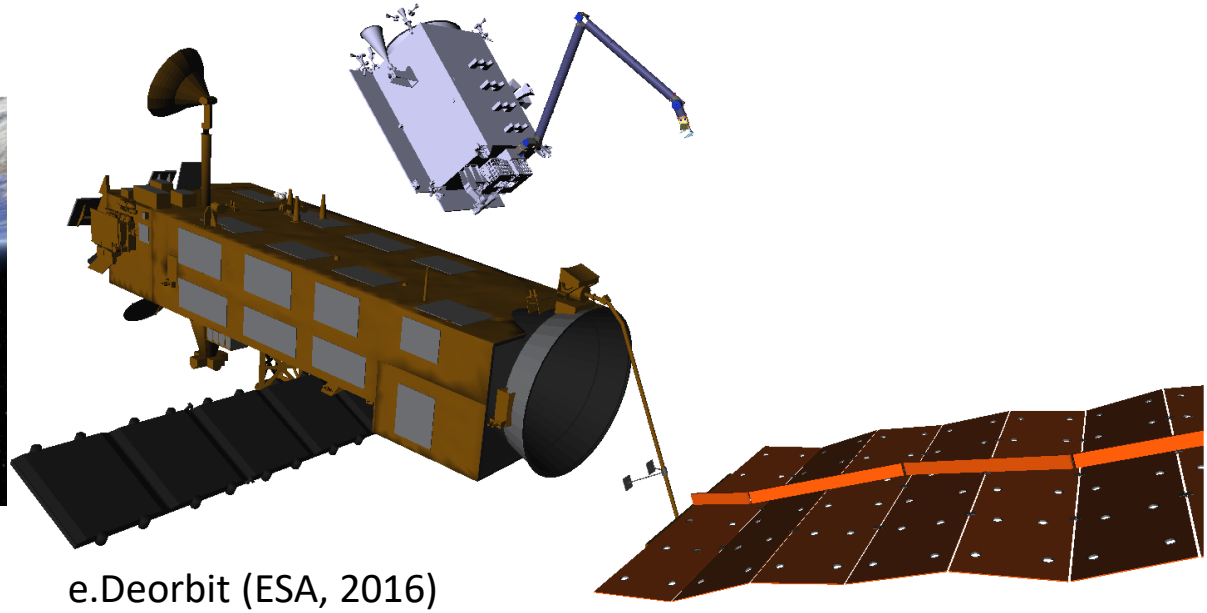
e.Deorbit (ESA, 2016)

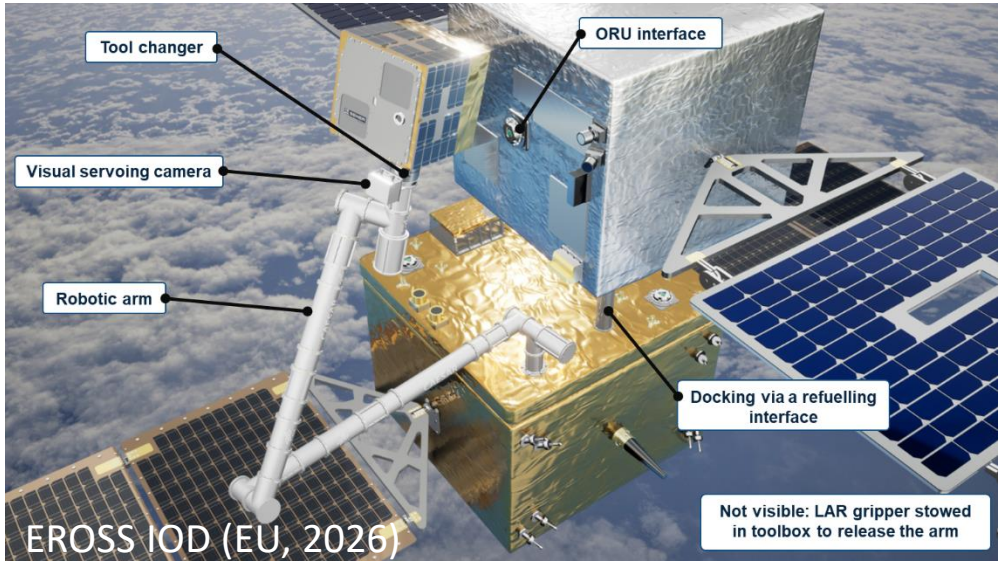

EROSS IOD (EU, 2026)

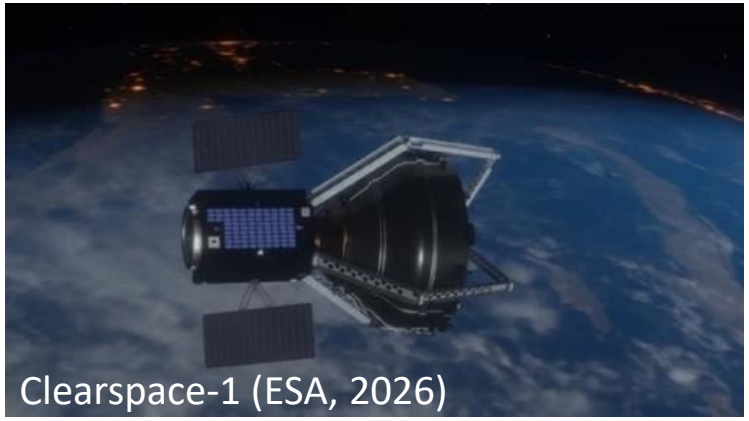
Clearspace-1 (ESA, 2026)

ADRAS-J
Astroscale

Conclusions

- Robotics is considered a key technology for accomplishing servicing tasks, the first of which is the capture of a defective target satellite. New scenarios include those in space stations.
- Dynamics of the potentially tumbling targets favors the implementation of autonomous operational procedures for performing the capture
- Autonomy for capture: target motion prediction, motion planning, tube-based MPC for tracking
- On-going research on robust parametric optimal control and its V&V

Thank you for your attention!